_IN-37_

_253131_

_108 p._

Mesh Refinement in Finite Element Analysis by Minimization of the Stiffness Matrix Trace

Madan G. Kittur and Ronald L. Huston
University of Cincinnati
Cincinnati, Ohio

November 1989

NASA
National Aeronautics and
Space Administration

US ARMY
AVIATION
SYSTEMS COMMAND
AVIATION R&T ACTIVITY

TABLE OF CONTENTS

1. INTRODUCTION

1.1　THE FINITE ELEMENT METHOD

The finite element method, in general, is an approximate method to solve differential equations. Using variational calculus the differential equation under consideration is posed as a functional. The resulting functional depends upon the unknowns and their derivatives with respect to the spatial coordinates x,y and z and possibly the time, t. In structural problems the functional represents a meaningful quantity, namely, the potential energy. However, in general, the functional may not have any physical interpretation. Minimizing the functional with respect to the unknowns is equivalent to solving the differential equation. The functional is minimized by setting its first variation to zero. In structural problems this corresponds to the well known concept of minimization of the potential energy. The result of the minimization is a set of algebraic equations

$$(1.1) \qquad [\,K\,]\{\,u\,\} = \{\,f\,\}$$

where [K] is the matrix of coefficients of the unknowns and is known as the

"stiffness matrix",

$\{ u \}$ is an array of unknowns and

$\{ f \}$ is an array of forcing functions.

The equations are then solved for u. In a typical application the domain under consideration is modeled by dividing it into elements. An interpolation function, or shape function, is set for the elements to interpolate values of the unknown at any point inside the element in terms of its values at the nodes. This interpolation function is used in the functional which when minimized as described above, yields the stiffness matrix. The reader is directed to several excellent books on finite element method by Zienkiewics [1,2]*, Segerlind [3], Reddy [4], and Huston [5]. The point to note for this report is the important role of the minimization process involved in the finite element methods.

1.2 MESH GENERATION

Each element in the finite element model is addressed by its

---

*Numbers in brackets indicate references listed at the end.

number. Also each node is addressed by its number. The inter-connectivity of the elements is determined by the common nodes shared by the elements. In a model with few elements and nodes, the user can manually divide the domain, number each element and node, and keep track of the element connectivity. However, in models with many nodes and elements, the effort required to divide the domain into elements and attend to connectivity is great. It then becomes difficult to accomplish this task without committing errors. However, there are several finite element pre-processors which do this job automatically once the geometry is defined. Users can then devote more time to interpreting results. Shephard [6] has reviewed the current trends in mesh generation. Although there are several ways to generate meshes, these methods fall into two broad categories:

1.2.1 MAPPING TECHNIQUES

This type of mesh generation is best suited when the geometry is simple - as in the case of a rectangle or a cuboid. Typically the user needs to choose the number of elements on each of the edges that defines the geometry and the element concentration along the edges. The software then generates the mesh simply by joining nodes on the opposite

3

edges. NASTRAN MSGMESH† , GIFTS□ , SUPERSAP● and SUPARTAB‡ (in I-DEAS) have this capability. For a more complicated geometry Schwarz-Christoffel [7] mapping has been used . The difficulty in evaluating integrals involved in the Schwarz-Christoffel transformation however makes this technique less attractive. Moreover, mesh generated by these techniques may introduce elements with high aspect ratios and elements that are highly distorted.

1.2.2 FREE MESH GENERATION

This method of generation is best suited for models with complicated geometry. SUPERTAB has this capability. The model is broken down into sub-areas and sub-volumes. On each of the curves of every sub-area and sub-volume the number of elements and their concentrations are selected. The software then generates a mesh that is consistent with the selected values and satisfies the requirement on the aspect ratios and the distortion factors of the elements.

---

† NASTRAN MSGMESH is developed by MacNeal-Schwendler Corporation
□ GIFTS is developed by Sperry Univac Computer System
● SUPERSAP is developed by Algor Corporation
‡ I-DEAS is developed by Structural Dynamic Research Corporation.

Although these pre-processors help in generating acceptable meshes, it is still difficult to obtain a mesh that is best suited for the problem at hand. The difficulty lies in the definition of the " best " mesh . Is there a best mesh for a particular domain ? If so, is there a different one for different set of boundary conditions or a different set of loading ? Is there a different optimal mesh for different differential equations in the same domain ? Answers to these questions are discussed in the following sections.

1.3 OPTIMAL MESH

Recall from section 1.1 that the functional is a function of the unknown or dependent variables. Note that it is also a function of the coordinates of the nodes. Therefore it can be expressed as:

(1.2) $\pi = \pi(u_i, d_k)$

where, u_i is the vector of unknown, d_k is the position vector of kth node.

In order to obtain a true minimum on (1.2), in addition to the equilibrium equations (1.1), it is necessary to consider the following

equations.

(1.3)

$$\frac{\partial \pi}{\partial d_k} = \frac{1}{2} u_i \frac{\partial K_{ij}}{\partial d_k} u_j - \frac{\partial f}{\partial d_k} u_i = r_k = 0$$

where, r_k is the residual vector.

Solution of (1.3) along with the geometrical constraints will yield the optimal locations of the nodes, which when used in (1.1) should result in a u_i that is closest to u_{exact}.

The method seems to be very simple, theoretically. However, the non-linear algebraic equations (1.3) are difficult to solve explicitly. Even for a simple geometry in one dimension the algebra is very complicated. Numerical solutions are also difficult [8]. Some of the solution methods for non-linear equations like gradient methods and complex methods have been tried but with little success. Among investigators examining this problem, Prager[9] has made a note worthy contribution. He examined a bar with a linearly varying cross section under tension. He showed that the grid producing the desired least potential energy is the one where the cross section areas at the nodes form a geometric series. This problem is studied in greater detail in the next chapter.

1.4 MESH REFINEMENT

As described in section 1.2 the user needs to select the number of nodes and elements in the model. The selection may be the one that leads to the best description of the domain geometrically. For example, a curved surface could be modelled by a series of interconnected flat rectangular facets. The larger the number of facets, the better is the model. The selection may also be based upon intuition, past experience and engineering judgement. The mesh obtained may be adequate in some cases. In other cases, especially when singularities are present, the mesh may not be adequate to obtain the results to the accuracy desired. In such cases, the meshes need to be refined.

1.4.1 REFINEMENT PROCESS

There are three ways of refining a finite element mesh:

a) The H-method: This method increases the number of elements and hence decreases the element size while keeping the polynomial order of the shape function constant.

b) The P-method: This method increases the polynomial order of

7

the interpolation function while keeping the number of elements in the model constant.

c) The R-method: This method redistributes the nodes while keeping the element number and the polynomial order of the interpolation function constant.

1.4.1.1 H - Method

This method is primarily based on the choice of characteristic length of the elements. "Characteristic length " is referred to in a generalized sense and is required to define the element topologically. A linear element requires one characteristic length, whereas an element of rectangular shape requires two characteristic lengths and a triangular element requires three characteristic lengths for its definition. In the triangular element the three length informations may be any combination of lengths and angles.

Instead of expressing the functional in terms of the position vectors of the nodes, as in (1.2), it can be expressed as a function of the element characteristic lengths as :

8

(1.4) $\qquad \pi = \pi(u_i, h_{lk})$

where, h_{lk} is the element characteristic length, l is the index on the characteristic length for element k

Also, note that there will be geometrical constraints on h_{lk}. For example, the sum of the element lengths in a particular direction should be equal to the overall dimension of the model in that direction. Again as described in section 1.3, the function can be minimized with respect to the characteristic lengths.

(1.5) $\qquad \dfrac{\partial \pi}{\partial h_{lk}} = \dfrac{1}{2} u_i \dfrac{\partial K_{ij}}{\partial h_{lk}} u_j - \dfrac{\partial f}{\partial h_{lk}} u_i = r_k = 0$

Solving (1.5) along with the constraints yield the characteristic lengths and hence defines the best mesh. Equation (1.5) is equivalent to (1.3) cast in the frame work of characteristic lengths. Therefore the solution as indicated in section 1.3 is difficult. A practical procedure using this method consists of selecting a coarse initial mesh, solving the equilibrium equations and computing the residue r_k on each element. The set of elements with large values of residues is the region that needs to be refined. The identified region can be refined by sub-dividing the elements, thus creating new regions, or by deleting all the elements in the

9

region and replacing them by finer elements. However, the new elements need to be of the same type as those in the initial mesh. The equations of the new model are solved and the residues are computed. If the values of the residues are still large, the refinement procedure can be repeated. Indeed , it could be used iteratively until the solution meets the prescribed accuracy.

The monotonic convergence of the refinement procedure has been studied by Melosh [10] and Key [11]. A convergence theorem has been introduced by Carroll and Baker [12], which states :

Theorem: A necessary consequence of the following refinement sequence

$$(1.6) \qquad \pi_n > \pi_{n+1} > \cdot \cdot \cdot > \pi_{n+m} \cdot \cdot \cdot > \pi_{exact}$$

where, m represents successive refinements of the initial finite element mesh n, is the existence of an optimum sub-division such that

$$(1.7) \qquad \pi_{n+m}(h_{lk}^*) < \pi_{n+m}(h_{lk})$$

where h_{lk}^* correspond to the optimum mesh.

The usefulness of this theorem can be explored in the discussion of the r - method. The difficulty in using this method is in the estimation of

the derivatives involved in the computations of the residues.

1.4.1.2 P - Method

This method is primarily based on the choice of the order of the interpolation function, which in practice, translates to the choice of element type. For example, in a two dimensional domain, the basic triangular element with three nodes at the three vertices uses a linear shape function (p=1). In order to choose quadratic shape functions (p=2), the triangular element with six nodes, three at the vertices and three at mid-side locations, has to be selected. Similarly, for cubic functions, an element with nine nodes is selected.

Higher order elements generally provide better description of the domain geometrically. They are particularly useful in regions where the use of lower order elements would result in a mesh with poor aspect ratios in those elements. From the point of view of solution accuracy, higher order elements are usually more accurate than the lower order elements. But this does not mean that increasing the polynomial order indiscriminately will always provide point-wise convergence to the exact solution. The argument is based on the theory of interpolation. Prenter [13] states that this notion on convergence was first dispelled by Meray and later by

Runge. He illustrates this with the function f(x) = 1/(1+5x2) being interpolated by Lagrange polynomial of order 5 and 15 with evenly spaced nodes in the interval [-1,1] which display divergence at - 1 and 1. Although the example is for a continuous interpolation function rather than a piecewise function, as in a finite element model, it shows that there is good reason to exercise caution in increasing the polynomial order.

1.4.1.3 R - Method

This is a far less explored method. It neither increases the polynomial order nor decreases the element character length. The mesh is refined simply by re-distributing the nodes in the domain such that the potential energy is reduced.

Recall the theorem introduced by Carroll and Baker, stated in section 1.4.1.1. The theorem indicates that there exists an optimal distribution of the nodes in a domain. Any other distribution will yield a potential energy higher than the lowest possible for the given number of degree of freedom. The theorem also indicates that : given a distribution of nodes, a new distribution will be a refinement over the old distribution

only if it results in a lower potential energy than the old distribution. This fact could be used in an iterative refinement procedures.

1.4.2 ADAPTIVE MESH REFINEMENT

The refinement that follows the requirements of the differential equation or the boundary conditions closely is called an adaptive refinement. This method is used to tailor the mesh, including finer elements. It can also provide elements of higher polynomial order where necessary as opposed to the method of h or p - refinement all over the domain. The practical method mentioned in section 1.4.1.1 is adaptive. The obvious advantage is that it achieves the desired accuracy level while keeping the number of degrees of freedom low.

1.4.3 A - PRIORI AND A - POSTERIORI METHODS

The classification of methods into a-priori and a-posteriori refers to refinement before and after the solution of the equilibrium equations. In a finite element program the solution process is one that needs much of computer time. If discretization errors can be estimated a-priori, then the mesh can be suitably altered to obtain the best accuracy possible by

solving the equations only once. Unfortunately there are no practical a-priori methods available. The author has not found any in the literature survey. This study is an attempt to provide one. There are several a-posteriori methods available for refinement.

1.4.4 USE OF HIERARCHICAL ELEMENTS IN REFINEMENT

An hierarchical displacement element is one whose stiffness matrix contains the stiffness matrices of lower order elements explicitly as submatrices[14].

Consider a two-node axial element. Its stiffness matrix is given by:

$$\frac{A\,E}{l} \begin{bmatrix} 1 & -1 \\ -1 & 1 \end{bmatrix}$$

An hierarchical displacement element of one higher order contains an additional node in the middle of the element, as in the conventional quadratic element. However the shape function chosen for the midside node is different from the one chosen in the conventional element. This results in the stiffness matrix:

$$\frac{A\,E}{l} \begin{bmatrix} 1 & -1 & 0 \\ -1 & 1 & 0 \\ 0 & 0 & \frac{16}{3} \end{bmatrix}$$

14

Note that the stiffness matrix of the basic element is contained in the new matrix as a submatrix. The stiffness matrices of higher order elements are built by a similar process if a higher order element is coded into the finite element program, it includes stiffness matrices of all lower order elements. In the process of refinement if a higher order element is chosen, the previously computed stiffness coefficients would still be valid. Hence, only a few additional coefficients have to be evaluated. The method is easier than the conventional p - method of increasing the polynomial order where the computation of the entire higher order element stiffness matrix is required.

Refinement using hierarchical elements is a-posteriori and appears to be attractive. However more research work needs to be done in this area.

1.5 RESEARCH OBJECTIVES

It is clear that the accuracy of the finite element results is mesh dependent. A proper mesh selection procedure is therefore necessary. A posteriori methods are adaptive in nature but are expensive in terms of computer processing time. On the other hand, a priori methods are not adaptive. They use geometrical criterions, element aspect ratios, for

15

example, for improvements. Some of them help estimating the overall error. They, however, do not indicate the regions which need refinement. The prime objective of this report is, therefore, to develop a criterion which helps in identifying the region for refinement or rezoning process even before the equilibrium equations are solved. The procedure based on the criterion should be able to guide the user in improving the grids.

Finally, the report itself is based upon the first author's doctoral dissertation [15] at the University of Cincinnati.

2. ANALYSIS

2.1 ANALYTICAL APPROACH

The objective is to develop a practical and efficient procedure of grid enhancement and optimization. The thesis is that for many problems the minimization of the trace of the stiffness matrix with respect to the nodal coordinates, leads to a minimization of the potential energy, and as a consequence, provides the optimal grid configuration. To see this, consider the governing matrix equation of finite element analysis:

$$(2.1) \qquad [K]\{u\} = \{f\}$$

where, $[K]$ is the stiffness matrix, $\{u\}$ is the array of dependent variables, and $\{f\}$ is the force array.

Matrix $[K]$ can be viewed as an operator which maps $\{u\}$ into $\{f\}$. In this context, since $[K]$ is symmetric, an orthogonal transformation $\{T\}$, which diagonalizes $[K]$, can be found. That is,

$$(2.2) \qquad [\hat{K}] = [T]^T[K][T]$$

where $[\hat{K}]$ is a diagonal matrix.

17

Let $[T]\{u\}$ and $[T]\{f\}$ be $\{\hat{u}\}$ and $\{\hat{f}\}$. Then the potential energy π may be expressed as:

$$(2.3) \qquad \pi = \frac{1}{2} \{u\}^T[K]\{u\} - \{f\}^T\{u\}$$

In terms of the array components, π becomes:

$$(2.4) \qquad \pi = \sum_{i=1}^{n}\left(\frac{1}{2} \hat{k}_{ii}\hat{u}_i^2 - \hat{f}_i\hat{u}_i \right)$$

where the $\hat{k}_{ii}$ (i=1,2,...,n) are the diagonal entries of $[\hat{K}]$.

Observe in Equation (2.4) that the last term: $\sum_{i=1}^{n}\hat{f}_i\hat{u}_i$ does not explicitly involve the nodal coodinates. Therefore, it does not effect the minimization of π with respect to the nodal coordinates. Also, since the u_i^2 are positive and are independent variables in the minimization of π, the minimization of π with respect to the nodal coordinates occurs when the sum of the $\hat{k}_{ii}$ (the trace of $[\hat{k}]$) is a minimum. Since the trace of a matrix is invariant under an orthogonal transformation, minimizing the trace of $[\hat{K}]$ is equivalent to minimizing the trace of $[K]$.

2.2 ENERGY APPROACH

Consider a one - degree of freedom system. The external work done ($=fu$) varies linearly with respect to u. Also the strain energy ($= 1/2\ Ku^2$) varies quadratically with respect to u. Potential energy is the difference of strain energy and work done. See Figure 2.1.

From the instant, the structure is loaded the operating point moves from the origin to the point where the potential energy reaches its minima (equilibrium).

Now consider the structure with a reduced stiffness ($K' < K$). The new strain energy and the potential energy curves are also shown in the figure. Note that the strain energy curve has become slightly flatter. Therefore the potential energy curve has reached a new low, which is lower than the previous. The displacement has improved from u_a to u_b. Therefore it is quite clear that in a single degree of freedom case, a less stiff structure has a lower potential energy than the stiff one.

Next, consider an n - degree of freedom system. Using an orthogonal transformation matrix, [K] can be diagonalized. This would decouple the degrees of freedom. Therefore each degree of freedom can be

19

compared with the single degree of freedom system as described above. If $[\hat{K}]$ is the transformed stiffness matrix, then finding minimum $\hat{k}_{ii}$ (i=1,2,...n) would yield the best grid. Since for the mesh configuration the minimum $\hat{k}_{ii}$ have been found, the trace of $[\hat{K}]$ which is the sum of $\hat{k}_{ii}$ will also be a minimum. But the trace is an invariant under orthogonal trasformation. Therefore minimization of trace of $[K]$ would lead to minimization of potential energy.

It should be noted that the diagonal dominance of $[K]$ is not adversely affected by the minimization of trace. The improved stiffness matrix is the result of redistribution of the nodes and of not any arbitrary mathematical operation.

Figure 2.1 - Strain Energy, Potential Energy and Work Done in a One Degree of Freedom System
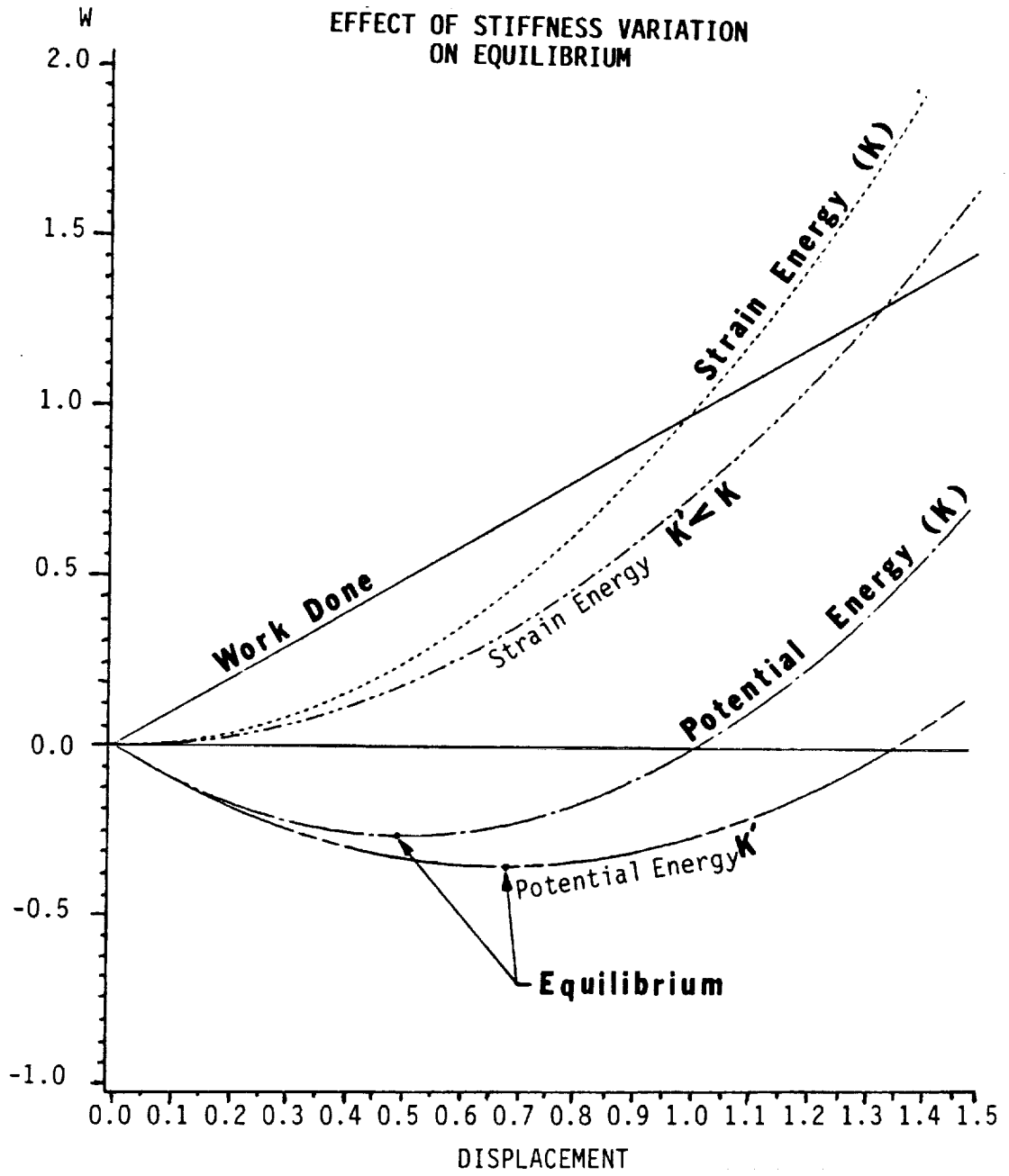
3. APPLICATIONS

Applications of concepts developed are illustrated in the examples in this chapter.

3.1 TAPERED BAR

3.1.1 DESCRIPTION

Consider the axially loaded tapered bar shown in Figure 3.1. (This is the same problem examined by Prager [9] and Masur [16]. The objective is to determine a finite element mesh which best predicts the axial displacement. Let the bar have length L and let it be divided into n elements with n+1 nodes (numbered 0 to n) as shown. Let the areas at the ends of the bar be A_o and A_1. Let ξ be the non dimensional length parameter defined as:

(3.1)
$$\xi = \frac{x}{L}$$

Then the area at any particular ξ along the bar is

(3.2) $\qquad A = A_0(1\text{-}c\xi)$

where c is

(3.3) $\qquad c = \dfrac{A_0\text{-}A_1}{A_0}$

Hence, the area at the ith node is:

(3.4) $\qquad A_i = A_0(1\text{-}c\xi_i)$

where, ξ_i is x_i/L.

Let the individual elements have a uniform cross section. For example, let the i_{th} element have cross section area $\overline{A}_i$ and length l_i as in Figure 3.2. (Note that the elements do not necessarily have the same length.) Then $\overline{A}_i$ and l_i are:

$$\overline{A}_i = \dfrac{A_{i\text{-}1}+A_i}{2}$$

(3.5)

$$l_i = x_i \cdot x_{i\text{-}1} = L(\xi_i \cdot \xi_{i\text{-}1})$$

The element stiffness matrix for the i_{th} element is [5] :

23

$$\text{(3.6)} \qquad [k] = \frac{\overline{A_i}E}{l_i} \begin{bmatrix} 1 & -1 \\ -1 & 1 \end{bmatrix}$$

where E is the elastic modulus. Then the trace τ of the global stiffness matrix is:

$$\text{(3.7)} \qquad \tau = 2E \sum_{i=1}^{n} \frac{\overline{A_i}}{l_i} = \frac{E}{L} \sum_{i=1}^{n} \left(\frac{A_{i-1}+A_i}{\xi_i - \xi_{i-1}} \right)$$

The improved node location occurs when the trace is minimized with respect to the nodal coordinates ξ_i (i=1,2,...n-1). Hence, by setting the derivative of τ with respect to ξ_i equal to zero we obtain:

(3.8)

$$\frac{\partial \tau}{\partial \xi_i} = 0 = \frac{E}{L} \left[\frac{\frac{\partial}{\partial \xi_i}(A_{i-1}+A_i)}{\xi_i - \xi_{i-1}} + \frac{\frac{\partial}{\partial \xi_i}(A_i+A_{i+1})}{\xi_{i+1}- \xi_i} - \frac{A_{i-1}+A_i}{(\xi_i - \xi_{i-1})^2} + \frac{A_i+A_{i+1}}{(\xi_{i+1}- \xi_i)^2} \right]$$

Using equation (3.5) and simplifying we obtain

(3.9)

$$A_{i+1} = A_i \left[\left(\frac{l_{i+1}}{l_i} \right)^2 - 1 \right] + A_{i-1} \left(\frac{l_{i+1}}{l_i} \right)^2 + cA_0 \left(\frac{l_{i+1}}{L} \right) \left[\left(\frac{l_{i+1}}{l_i} \right) + 1 \right]$$

To simplify the analysis it is convenient to introduce the length ratio

24

parameter r_{ij} defined as l_i/l_j. Then the ratio l_{i+1}/l_i may be written as:

$$(3.10) \qquad \frac{l_{i+1}}{l_i} = \frac{\dfrac{l_{i+1}}{l_1}}{\dfrac{l_i}{l_1}} = \frac{r_{i+1,1}}{r_{i1}}$$

Then L/l_i is

$$(3.11) \qquad \frac{L}{l_i} = \sum_{j=1}^{n} \frac{l_j}{l_i} = \sum_{j=1}^{n} \frac{r_{j1}}{r_{i1}} = \frac{S_n}{r_{i1}}$$

where S_n is defined as $\displaystyle\sum_{j=1}^{n} r_{j1}$.

Using this notation Equation (3.9) may be rewritten as

$$(3.12)$$

$$A_{i+1} = A_i \left[\left(\frac{r_{i+1,1}}{r_{i1}} \right)^2 - 1 \right] + A_{i-1} \left(\frac{r_{i+1,1}}{r_{i1}} \right)^2 + \frac{cA_0 r_{i+1,1}}{S_n} \left[\left(\frac{r_{i+1,1}}{r_{i1}} \right) + 1 \right]$$

Also, ξ_i may be written as:

$$(3.13) \qquad \xi_i = \frac{l_1 + l_2 + \cdots + l_i}{L}$$

25

$$\xi_i = \frac{1 + r_{21} + r_{31} + \cdots + r_{i1}}{S_n}$$

$$= \frac{1}{S_n} \sum_{j=1}^{i} r_{j1} = \frac{S_i}{S_n}$$

Then, from equation (3.4), A_i may be written as

(3.14)
$$A_i = A_0 \left[1 - c \left(\frac{S_i}{S_n} \right) \right]$$

Specifically, A_1 and A_2 are

$$A_1 = A_0 \left[1 - \left(\frac{c}{S_n} \right) \right]$$

(3.15)

$$A_2 = A_0 \left[1 - c \frac{(1 + r_{21})}{S_n} \right]$$

To obtain the element area ratios let i=1 in equation (3.12). A_2 is then

(3.16)
$$A_2 = A_1 \left(r_{21}^2 - 1 \right) + A_0 r_{21}^2 + c A_0 r_{21} \left(\frac{r_{21} + 1}{S_n} \right)$$

Then, by using equations (3.15) to eliminate A_1 and A_2, we obtain

$$(3.17) \qquad S_n(1 - r_{21}) = c$$

From the first of equations (3.15) we have

$$A_1 = A_0 r_{21}$$

$$(3.18) \qquad \text{or}$$

$$\frac{A_1}{A_0} = r_{21}$$

Similarly, the second of equations (3.15) leads to

$$A_2 = A_0 r_{21}^2$$

$$(3.19) \qquad \text{or}$$

$$\frac{A_2}{A_1} = r_{21}$$

Next, let i=2 in equation (3.12). By using the same procedure we obtain

$$(3.20) \qquad 1 - r_{32} = \frac{c}{S_n} (1 - r_{32} + r_{21})$$

But, in view of equation (3.17) this becomes

$$1 - r_{32} = (1 - r_{21}) (1 - r_{32} + r_{21})$$

(3.21)   or

$$r_{21}(r_{32} - r_{21}) = 0$$

Thus,

(3.22) $$r_{32} = r_{21}$$

From equation (3.14) we have

(3.23) $$A_3 = A_0 \left[1 - c \left(\frac{S_3}{S_n} \right) \right] = A_0 r_{21}^3$$

Therefore, we obtain

(3.24) $$\frac{A_3}{A_2} = \frac{A_2}{A_1} = \frac{A_1}{A_0} = r_{21} = r_{32}$$

Proceeding similarly for i=3,4,...   we get

$$\frac{A_n}{A_{n-1}} = \frac{A_{n-1}}{A_{n-2}} = \cdots = \frac{A_1}{A_0} = r_{21} = r_{32} = \cdots = r_{n,n-1}$$

Thus, we have the relations

$$r_{31} = r_{21}r_{32} = r_{21}^2$$

(3.26)

$$r_{41} = r_{43}r_{32}r_{21} = r_{21}^3$$

$$r_{i1} = r_{21}^{i-1}$$

Hence, S_i is the geometric series

(3.27)

$$S_i = 1 + r_{21} + r_{21}^2 + \cdots + r_{21}^{i-1} = \frac{1 - r_{21}^i}{(1 - r_{21})}$$

Then, from equations (3.14) and (3.17), we have

$$A_i = A_0\left[1 - (1 - r_{21}^i)\right] = A_0 r_{21}^i$$

(3.28)   and then

$$A_n = A_0 r_{21} = A_1$$

29

Then, from equation (3.3) we see that r_{21} is

(3.29) $$r_{21} = (1 - c)^{1/n}$$

Finally, by substituting into equation (3.13) we have

$$(3.30) \quad \xi_i = \frac{l_1}{L} (1 + r_{21} + r_{31} + \cdots + r_{i1})$$

$$= (1 - r_{21}) \left[\frac{1 + r_{21} + r_{21}^2 + \cdots + r_{21}^{i-1}}{c} \right]$$

$$= \frac{1 - r_{21}^i}{c} = \frac{1 - (1 - c)^{i/n}}{c}$$

This is the result obtained by Prager [9] in his analysis of the same problem.

3.1.2 DISCUSSION

First, observe that in Equation (3.30) for a uniform thickness beam c is zero and thus ξ_i is undetermined. This means that for a uniform

thickness beam the nodal position are arbitrary. That is, all mesh are equally optimal for a uniform thickness beam.

Next, consider again the element stiffness matrix of equation (3.6). From equations (3.4) and (3.30) the scalar multiplier is

$$(3.31) \qquad \frac{E\overline{A}_i}{l_i} = \frac{E(A_{i-1} + A_i)}{2L(\xi_i - \xi_{i-1})} = \frac{A_0 c}{2L}\left[\frac{1 + r_{21}}{1 - r_{21}}\right]$$

Since this is a constant (independent of i) the element stiffness matrix is the same for each element. This means that each element has the same strain energy. Masur [15] has suggested that this result is due to the simple geometry of the problem.

Even with this simple geometry however, like the methods discussed in section 1.3, the analysis needed to determine the optimal nodal positions has been extremely detailed. With more complex geometries the analysis will become intractable. However, it is not necessary to obtain recursive relationships by analytical methods as employed in this example. The criteria of minimizing the trace of the stiffness matrix is a comparatively simple procedure - readily amenable to the development of computer algorithms for optimal nodal locations.

3.1.3 NUMERICAL EXAMPLE

To illustrate the value of optimizing the mesh consider an axially loaded bar which tapers to 1/3 the base area as in Figures 3.1 to 3.3. Specifically, let P, A_o, C, E, and L have the values:

$$(3.31) \qquad P = 20N, \quad A_o = 0.0015m^2, \quad C = 2/3$$

$$E = 2.07 \times 10^{11}N/m^2, \quad L = 4m$$

The objective is to find the axial displacement. From elementary mechanics the axial displacement u at any location x is:

$$(3.33) \qquad u = -\frac{PL}{A_o Ec} \ln\left[1 - \frac{cx}{L}\right]$$

To compare the displacement results of finite element models with Equation (3.33), four models of the bar, each having four elements, were examined. One of the models had a uniform nodal distribution. Another had the "optimal" mesh as developed in Equation (3.33). The remaining two models had arbitrarily selected nodal distributions. The nodal displacements were evaluated using the four models and compared with

32

the displacements calculated by (3.33). Table 3.1 shows the results. Table 3.2 presents an error analysis and also an L_2 - norm of the error. As expected the optimum mesh produces the least L_2 error.

TABLE 3.1 - Comparison Of Axial Displacements For The Tapered Bar Of Figure 3.1 Calculated Using Various Models

Axial location x, m	Exact displacement eq. (3.30), 10^{-9}m	Displacements using various models, 10^{-9}m			
		Uniform Mesh	"Optimum" Mesh (Prager)	Mesh 3	Mesh 4
0.0	0.0	0.0	0.0	0.0	0.0
0.5	33.6276			33.60639	33.60639
1.0	70.46244	70.2679		70.41338	
1.4409860	106.1461		105.4820		
2.0	156.7020	156.1509			15.56506
2.5	208.3078			206.8158	207.1804
2.5358986	212.2923		210.9648		
3.0	267.8830	266.5719			
3.3678522	318.4384		316.4529		
4.0	424.5845	421.1612	421.940	417.6195	417.9814

TABLE 3.2 - Error Analysis (Tapered Bar)

Axial location x, m	Error for various meshes, 10^{-9} m			
	Uniform mesh	"Optimum" mesh (Prager)	Mesh 3	Mesh 4
0.0	0.0	0.0	0.0	0.0
0.5			0.02121	0.02121
1.0	0.1945411		0.04906	
1.4409860		0.664118		
2.0	0.5506105			1.0514
2.5			1.492	1.1274
2.5358986		1.32769		
3.0	1.311108			
3.3678522		1.985439		
4.0	3.423228	2.64433	6.965	6.6031
l_2 - norm	3.7119418	3.6246009	7.1232118	6.780697

3.1.4 OBSERVATIONS

[1] The analysis and the numerical results demonstrate the potential usefulness of the trace minimization mesh improvement method.

[2] Minimization of the trace of the stiffness matrix is a relatively simple mesh optimization procedure. It is readily adaptable to algorithm development.
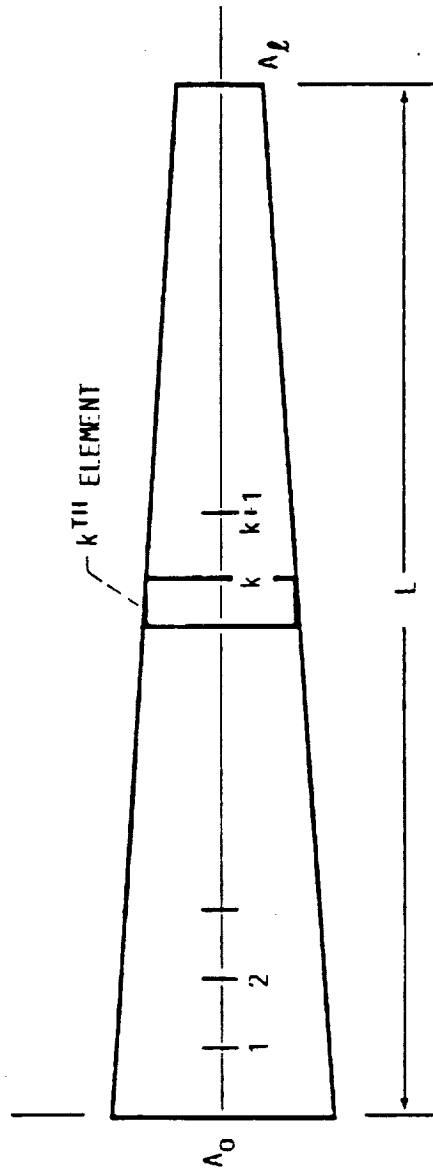
Figure 3.1 - Tapered Bar
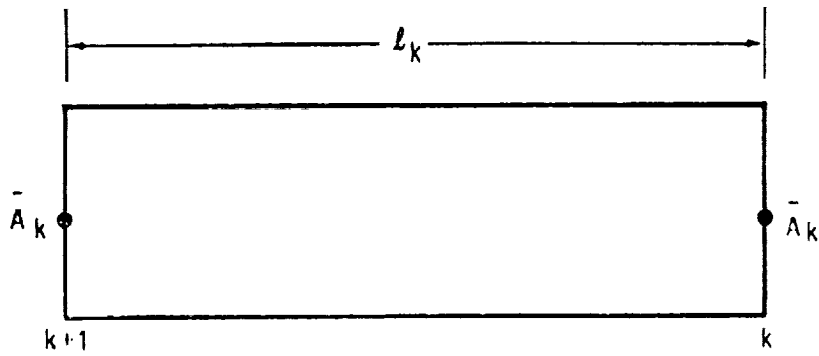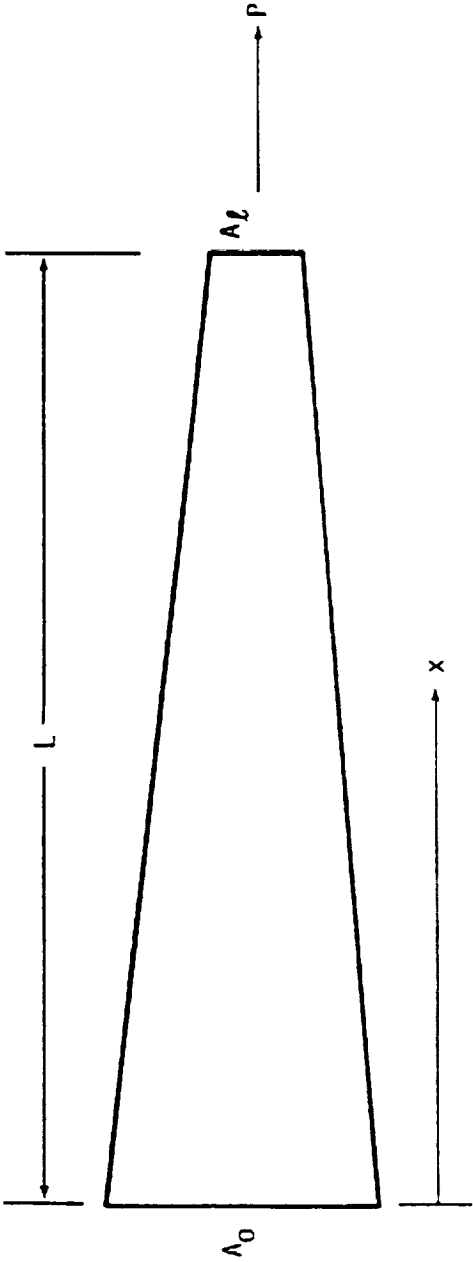
Figure 3.2 - Element in the Tapered Bar Model

Figure 3.3 - Tapered Bar with Axial Load

3.2 HEAT TRANSFER IN AN INFINITE CYLINDER

3.2.1 CONFIGURATION AND PROBLEM DEFINITION

Consider an annular cylinder with infinite length having inner and outer radii: r_o and r_n. Let the thermal conductivity be κ. Let the temperatures at the inner and outer radii be: T_o and T_n. Then the governing equation for the temperature distribution along a radial lines is:

$$(3.34) \qquad \frac{d}{dr}\left[r\kappa\frac{dt}{dr} \right] = 0$$

The boundary conditions are:

$$(3.35) \qquad T = T_0 \qquad \text{at} \quad r = r_0$$

$$T = T_n \qquad \text{at} \quad r = r_n$$

The solution of equation 3.34 subject to equation 3.35 is:

$$(3.36) \qquad T = T_n + (T_0 - T_n)\frac{\ln\left(\dfrac{r_n}{r}\right)}{\ln\left(\dfrac{r_n}{r_0}\right)}$$

Next, suppose that the temperature gradient at the inner surface is specified as: q_0. The boundary conditions are then:

$$(3.37) \qquad \frac{dT}{dr} = q_0 \qquad \text{at} \quad r = r_0$$

$$T = T_n \qquad \text{at} \quad r = r_n$$

In this case the solution of equation 3.34 is:

$$(3.38) \qquad T = T_n - r_0 q_0 \ln\left(\frac{r_n}{r}\right)$$

3.2.2 FINITE ELEMENT FORMULATION AND MESH OPTIMIZATION

Figure 3.4 shows the finite element model. It consists of a series of annular elements. For elements (e) let the inner and outer radii be r_e and r_{e+1}. The entries of the stiffness matrix are:

$$(3.39) \qquad k_{ij}^e = 2\pi\kappa_e \int_{r_e}^{r_{e+1}} r \left(\frac{dN_i^e}{dr}\right) \left(\frac{dN_j^e}{dr}\right) dr$$

where κ_e are the element conductivity constants and where the element shape functions N_i^e and N_j^e are:

$$(3.40) \quad N_i^e = \frac{\left(r_{e+1} - r \right)}{\left(r_{e+1} - r_e \right)} \quad \text{and} \quad N_j^e = \frac{\left(r - r_e \right)}{\left(r_{e+1} - r_e \right)}$$

By carrying out the indicated operations the element stiffness matrix becomes:

$$(3.41) \qquad \left[k_{ij}^e \right] = S_e \begin{bmatrix} 1 & -1 \\ -1 & 1 \end{bmatrix}$$

where S_e is defined as:

$$(3.42) \qquad S_e = \pi \kappa_e \frac{r_e + r_{e-1}}{e_e - r_{e-1}}$$

Hence the trace τ, of the global stiffness matrix is:

$$(3.43) \qquad \tau = 2 \sum_{e=1}^{n} S_e$$

where n is the the number of elements.

The trace may be minimized with respect to the nodal coordinates by setting the partial derivative of τ with respect to r_e, equal to zero. This leads to the relatively simple relation:

$$(3.44) \qquad \frac{r_{e+1}}{r_e} = \frac{r_e}{r_{e-1}}$$

By repeated use of this relation the nodal positions are given by:

$$(3.45) \qquad r_e = r_0 \left(\frac{r_n}{r_0}\right)^{e/n}$$

3.2.3 NUMERICAL EXAMPLES

To illustrate the effectiveness of the method considers the annular cylinder with the following temperatures specified on the boundaries:

$$(3.46) \qquad r_0 = 20 \text{ mm} \qquad T_0 = 100^\circ \text{ C}$$

$$r_n = 50 \text{ mm} \qquad T_n = 0^\circ \text{ C}$$

Let the conductivity be constant throughout the cylinder with value: 1.0.

Consider two finite elements models, each with four elements: Let the first have a uniformly spaced mesh. Let the second have a mesh with nodal spacing governed by equation 3.45. The objective is to determine the temperature distribution across the thickness.

The solution of the finite element governing equations lead to the results listed in Table 3.3. (The temperatures at the intermediate points, if they are not obtained directly, are obtained using linear interpolation between the nodal values.) The error is defined as the difference between the theoretical results and the finite element results. The mesh governed by equation 3.34 (called the "improved" mesh) is found to have zero errors at the nodes. Hence, the L_2 norm of the errors* is much smaller than that of the uniform mesh.

TABLE 3.3 - Comparison Between Finite Element Uniform Mesh and Improved Mesh Temperature Results with Theoretical Values for Temperature Specified Boundary Conditions

Radius (mm)	Temperature ° C			Error	
	Uniform Mesh	Improved Mesh	Theoretical Values	Uniform Mesh	Improved Mesh
20.0	100.0	100.0	100.0	0.0	0.0
25.148669	76.21655	75.0	75.0	-1.216559	0.0
27.5	65.354967	65.920251	65.24534	-0.109625	-0.674909
31.622777	50.881148	50.0	50.0	-0.881148	0.0
35.0	39.024743	39.628662	38.92596	-0.098784	-0.702703
39.763536	25.538185	25.0	25.0	-0.538185	0.0
42.5	17.790692	18.316874	17.73661	-0.05408	-0.580262
50.0	0.0	0.0	0.0	0.0	0.0
L_2 norm of error :				1.6033656	1.1340184

Next, consider the same cylinder but let the temperature gradient be specified on the inner boundary. Specifically, let the boundary conditions be:

$$(3.46) \qquad \frac{dT}{dr} = -5.4567833 \text{°C/mm at } r_o = 50 \text{ mm}$$

$$T = T_n = 0°C \qquad\qquad \text{at } r_n = 50 \text{ mm}$$

(The temperature gradient of -5.4567833 ° C/mm on the inner boundary leads to the same theoretical temperature distribution as in the first

example.) Table 3.4 shows the comparisons between the finite element solutions and the theoretical values of the temperature. Once again the L_2 norm of the error shows that the improved mesh provides better results than the uniform mesh.

TABLE 3.4 - Comparison Between Finite Element Uniform Mesh and Improved Mesh Temperature Results with Theoretical Values for Temperature / Temperature Gradient Specified Boundary Conditions

Radius (mm)	Temperature °C			Error	
	Uniform Mesh	Improved Mesh	Theoretical Values	Uniform Mesh	Improved Mesh
20.0	99.47716	99.570031	100.0	0.52284	0.42997
25.148669	75.818072	74.677527	75.0	-0.818072	0.322473
27.5	65.01327	65.636818	65.24534	0.23207	-0.391478
31.622777	50.615125	49.78502	50.0	-0.615125	0.214981
35.0	38.82071	39.458273	38.92596	0.10525	-0.532313
39.763536	25.404668	24.892511	25.0	-0.404668	0.10749
42.5	17.69768	18.238117	17.73661	0.03893	-0.501507
50.0	0.0	0.0	0.0	0.0	0.0
L_2 norm of error :				1.245467	1.0172293

Since the temperature gradient is specified at the inner boundary, it is also of interest to know how the values of the temperature gradients obtained using the two finite element meshes compare with each other

and with the theoretical values. Table 3.5 provides such a comparison. (the temperature gradients at the intermediate points, if they are not obtained directly, are computed by using forward differences.) The improved mesh has a small error at the inner radius as well as a smaller L_2 norm of errors overall.

3.2.4 DISCUSSION

The numerical example show that the "improved" mesh of equation 3.45 produces results which are closer to the theoretical values than those obtained using the uniform mesh. Therefore, the mesh of equation 3.45 is an improvement over the uniform mesh for both the temperature fixed boundary conditions and for the mixed boundary conditions.

The values of stiffness matrix traces of the uniform and improved meshes are 74.666666 and 70.151974 respectively. This indicates that for these examples the trace is not especially sensitive to the nodal locations. Therefore, the difference in the L_2 norms of error are not great. More dramatic difference in the results will occur in problems where the trace is more sensitive to changes in the nodal positions.

TABLE 3.5 - Comparison Between Finite Element Uniform Mesh and Improved Mesh Temperature Gradient Results with Theoretical Values for Temperature / Temperature Gradient Specified Boundary Conditions

Radius (mm)	Temperature °C			Error	
	Uniform Mesh	Improved Mesh	Theoretical Values	Uniform Mesh	Improved Mesh
20.0	-4.5951853	-4.8347453	-5.4567833	0.861598	0.622038
25.148669	-4.5951853	-3.8449325	-4.3396146	-0.2555571	-0.4946821
27.5	-3.4923413	-3.8449325	-3.9685697	0.4762284	0.1236372
31.622777	-3.4923413	-3.0577627	-3.4511702	-0.0411711	-0.3934075
35.0	-2.816404	-3.0577627	-3.1181619	0.3017579	0.0603992
39.763536	-2.816404	-2.4317489	-2.7446192	-0.0717848	-0.3128703
42.5	-2.3596907	-2.4317489	-2.567898	0.2082073	0.1361491
50.0	-2.3596907	-2.4317489	-2.1827133	-0.1769774	-0.2490356
L_2 norm of error on gradients :				1.0986497	0.9918611

In summary, the results obtained in this paper confirm that nodal positioning by minimizing the stiffness matrix trace leads to either an optimum or near-optimum mesh. If the mesh is not optimum it can be a starting mesh for other mesh refinement procedures and for procedures using element division or element enhancement (h-methods or p-methods).

Figure 3.4 - Finite Element Model of the Cylinder (Heat Transfer)
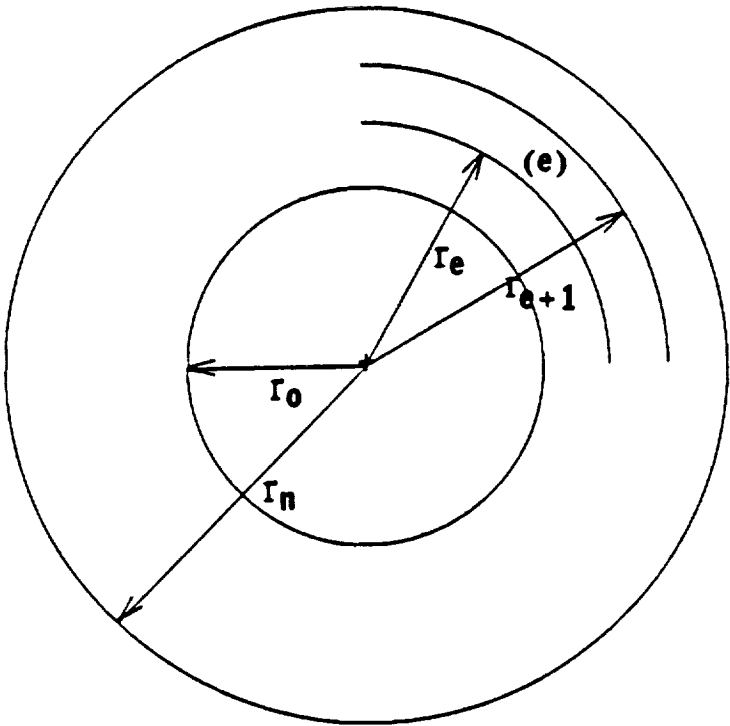
3.3 AIRCRAFT LUG PROBLEM

3.3.1 INTRODUCTION

Accuracy and reliability of finite element computation are among the most important considerations in numerical structural analysis. Run time and costs are becoming less important. Indeed, the costs incurred in ensuring that the results are accurate are negligible as compared with the costs of potential consequence of wrong decisions [17].

In accurate finite element modelling, a combination of element size modification (h-refinement) and element order modification (p-refinement) provide the most efficient solution convergence. An exponential rate of convergence can be achieved with optimally designed meshes and optimal order refinements, [18,19]. From a practical standpoint, however, it is often difficult to implement and achieve exponential convergence. Nevertheless, Szabo [17] states that "good" results can be obtained through mesh design along with element order refinements.

The most widely used procedure is to:

[1]   Select large elements where the solution is known to be smooth.

[2]   Select smaller elements where the solution is known to vary rapidly; as around points of singularity.

Szabo suggests that refinement toward the singularity should be in geometric progression with the ratio of sizes of about 0.1 to 0.15. These are empirical values. When small size ratios are used, bad element aspect ratios are often introduced leading to poor mesh design. Extreme element aspect ratios are the cause for overestimation of structural stiffness [19].

The intention of this study is to find a rationale which will guide the analyst in selecting a good mesh. The procedure developed herein has shown that an improved mesh can be obtained by minimizing the trace of the stiffness matrix. The conventional procedure, as outlined above, is used in initial mesh selection. The mesh is then improved by minimizing the stiffness matrix trace by moving the grid point locations. The "improved" mesh can then be used in the h or p-version of mesh refinement leading to a much faster convergence. It is believed that the effort spent in minimizing the trace will be rewarded in convergence of the solution after fewer h or p iterations.

3.3.2 ANALYSIS

Convergence of finite element solutions are often measured by the value of the total strain energy. With improvements in grid, the total strain energy usually increases. Mesh improvements based on the total strain energy produces convergence in the average sense. An analyst, however, generally wants to know the location and the accurate value of the maximum stress as well as accurate values of displacement at designated points as dictated by design requirements.

If u is the actual displacement field and if û is the displacement predicted by the finite element method, then $||u - û||$ is the norm of error on displacement. Since the displacement formulation of the finite element method renders the structure overstiff, u is larger than û. Therefore û converges from below. Hence, from a practical standpoint, a combined displacement, stress and strain energy criterion should be used.

In his study [17] Szabo has used hierarchical basic functions for interpolation and has demonstrated p-version convergence in an analysis of an aircraft lug as shown in Figure 3.5. The lug is 0.5 inches thick and the rest of the dimensions, as shown, are in inches. It is made of isotropic material of modulus of elasticity of 30,000 ksi and Poisson's ratio of 0.3. The lug is fixed along AB. A circular pin carrying a load of 10.0 kips,

inclined at an angle of 45 degrees to the horizontal, fits tightly in the hole of the lug and exerts pressure on it. The results of total strain energy changes obtained in Szabo's modellings are listed in Tables 3.6 and 3.7 for easy comparison.

In the present study, the standard QUAD4, QUAD8, TRIA3 and TRIA6 elements of MSC - NASTRAN are used. The mesh used by Szabo is shown in Figure 3.6. Note that elements 2 and 11 are distorted. In attempting to improve the mesh, grid point 8 is moved to a new location as shown in Figure 3.7. Next, grid points 2,3,5 and 6 are moved to obtain the mesh of Figure 3.8. Table 3.6 shows the effect upon the total strain energy along with the reduction in the stiffness matrix trace. (The trace of the stiffness matrix is obtained by using a series of DMAP instructions of MSC-NASTRAN as indicated in the Appendix.) This improvement is significant when compared with results of Szabo (see Tables 3.6 and 3.7) for the same number of degrees of freedom. (English units are employed in the tables.)

TABLE 3.6 - Comparison of Performance of Meshes 1,2 and 3

	Mesh 1	Mesh 2	Mesh 3
Trace (* 10^5)	8.0856	7.8712	7.5158
Degrees of Freedom	36	36	36
Strain Energy(* 10^{-2})	1.966856	2.068929	2.179273
Displacement at node 12 (* 10^{-3})	5.52766	5.92351	6.39045
Von-Mises Stress			
at node 1	18.15	18.5	15.30
at node 4	23.42	24.5	20.51
at node 18	5.663	5.641	5.618
Max.Prin. Stress			
at node 1	-2.056	-3.446	-2.364
at node 4	25.3	26.89	22.24
at node 18	4.97	4.731	4.696
Min.Prin. Stress			
at node 1	-19.09	-19.98	-16.34
at node 4	4.361	5.803	4.092
at node 18	-1.195	-1.513	-1.528

The maximum vertical displacement occurs at the tip of the lug (node 12). In Table 3.6 it is seen that the lower value of trace is associated with a higher maximum displacement (node 12). Since finite element models tend to present "stiffer than actual" systems, the trace minimization demonstrates the mesh improvement. In mesh 2 since only grid point 8 is moved to lower the value of trace, the stress values at nodes 1 and 4 are more accurate than those predicted by mesh 1. In mesh 3, elements 1 and 3 are larger than those of mesh 1. Therefore, their centroids are farther away from nodes 1 and 4 which leads to lower stress estimation at those nodes. Thus, an improved displacement value is obtained at the

expense of stress values. This indicates that the mesh near nodes 1 and 4 needs to be refined. Mesh 3 can of course be improved by further minimization of the trace.

TABLE 3.7 - Variation of Strain Energy with P-Refinement.

Polynomial Order	Degrees of Freedom	Strain Energy ($* 10^{-2}$)
1	36	1.73592
2	100	2.76935
3	170	2.83543
4	266	2.85719
5	388	2.86491
6	536	2.86839
7	710	2.86906
8	910	2.86928

Next, mesh 1 is refined by increasing the polynomial order to 2 to obtain mesh 1a. Mesh 4 is constructed by refining mesh 3 using an h-version modification catering to the regions of high stress around nodes 1 and 4 and around the hole.

When singularities are not present, an increase in p will result in an increase in the rate of convergence. However, if singularities are present, p-refinement, with a given mesh, will not necessarily result in an indefinite increase in the rate of convergence. However an optimal rate of convergence can be obtained by a proper spacing of the mesh around the

singularity [26]. Further mesh 4 is improved by reducing the trace of the stiffness matrix to obtain mesh 5. Results of the three meshes are listed in Table 3.8.

TABLE 3.8 - Comparison of Performance of Meshes 1a, 4 and 5.

	Mesh 1a	Mesh 4	Mesh 5
Trace (* 10^5)	43.166	32.577	31.402
Degrees of Freedom	100	96	96
Strain Energy(* 10^{-2})	2.994742	2.448802	2.440627
Displacement at node 12 (* 10^{-3})	9.02065	7.32149	7.33578
Von-Mises Stress			
at node 1	20.14	23.34	23.76
at node 4	26.79	30.62	31.13
at node 18	15.22	22.45	20.35
Max.Prin. Stress			
at node 1	-5.086	-5.737	-5.978
at node 4	29.46	33.77	34.38
at node 18	16.6	22.27	20.54
Min.Prin. Stress			
at node 1	-22.19	-25.68	-26.18
at node 4	6.552	7.805	8.1
at node 18	3.326	-0.344	-0.378

Note that these meshes have almost the same number of degrees of freedom and therefore their performances can be compared with each other. Since quadratic interpolation is is generally more accurate than linear interpolation, mesh 1a predicts an improved strain energy value compared to the other two. However, since the region around nodes 1 and 4 and also around the hole have small elements in mesh 4 and 5,

the stress values predicted are much higher than those of mesh 1a. Also, the displacement values are improved. The trace in mesh 5 is smaller because the elements around the hole are less distorted as compared with those of mesh 4. This leads to a larger displacement but at the expense of a lower stress prediction around the hole. However, since a smaller trace improves the mesh in the overall sense, the stress values at 1 and 4 are higher. It should also be noted that the strain energy of mesh 5 is smaller than that of mesh 4.

The convergence of finite element results in the energy norm is not monotonic [28]. However, a larger displacement indicates a larger work done by external loads and consequently a lower potential energy. Again mesh 5 could be improved by relocating the nodes to lower the trace.

Next, mesh 5a is constructed by increasing the polynomial order of mesh 5 to two. Table 3.9 can be used for a comparative study of the three meshes: mesh 1 used by Szabo, mesh 1a obtained by a p-extension of mesh 1, and mesh 5a obtained by combined h and p-extension along with the improvement procedure based on trace minimization.

Increases in stress values of mesh 5a from those of mesh 1 vary from 40% to 400%. Also, the increase in displacement is 65%. This shows

the need for refinements and improvements. A large strain energy value of mesh 1a indicates that a p- version refinement converges faster on an average sense. Higher stress values of mesh 5a indicate the superiority of the h-version refinement. Moreover, the h-version may introduce distorted elements. To obtain the best overall mesh for a given number of degrees of freedom, it is therefore useful to improve the mesh by trace minimization procedure.

Conclusions:

In view of the foregoing results a combined stress, displacement and strain energy criterion should be used to monitor the convergence. A combined grid improvement and refinement procedure should be used for the best results.

The study confirms that the h and p-extensions lead to improved meshes. The study also shows that the stiffness matrix trace is a good measure of the quality of a mesh, especially when singularities are present. Therefore, the step by step procedure to be followed by an analyst is:

[1]   Select large elements where the solution is known to be smooth.

[2] Select smaller elements where the solution is known to vary rapidly.

[3] Improve the grid by reducing the stiffness matrix trace.

[4] Perform a numerical solution.

[5] Refine the grid by using the h-version refinement and by introducing smaller elements in high stress areas.

[6] Improve the grid as in step 3.

[7] Refine the grid using the p-version refinement.

[8] Continue to iterate until the convergence criterion is satisfied.

TABLE 3.9 - Comparison of Performance of Meshes 1, 1a and 5a.

|	Mesh 1	Mesh 1a	Mesh 5a
Trace (* 10^5)	8.0856	43.166	158.43
Degrees of Freedom	36	100	322
Strain Energy(* 10^{-2})	1.966856	2.994742	3.020364
Displacement at node 12 (* 10^{-3})	5.52766	9.02065	9.10035
Von-Mises Stress			
at node 1	18.15	20.14	25.25
at node 4	23.42	26.79	33.71
at node 18	5.663	15.22	23.48
Max.Prin. Stress			
at node 1	-2.056	-5.086	-5.897
at node 4	25.3	29.46	36.91
at node 18	4.97	16.60	23.90
Min.Prin. Stress			
at node 1	-19.09	-22.19	-27.68
at node 4	4.361	6.552	7.768
at node 18	-1.195	3.326	-0.872

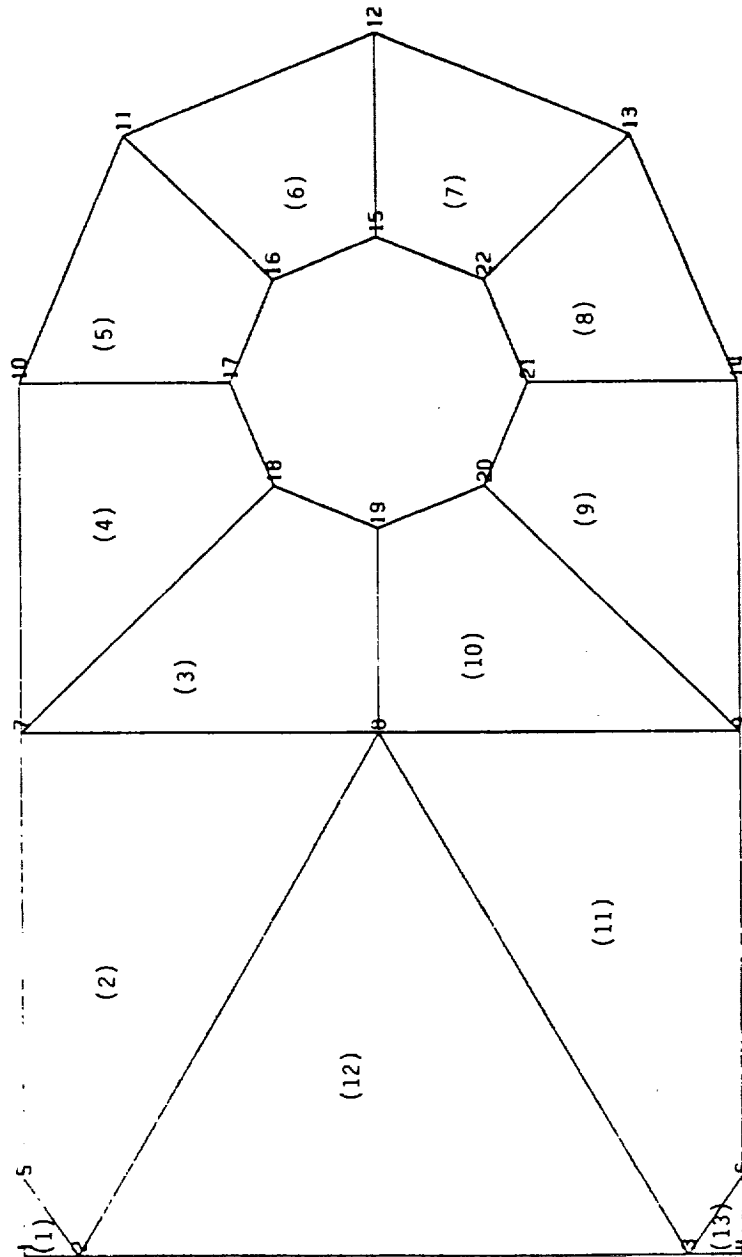**Figure 3.5 - Aircraft Lug**
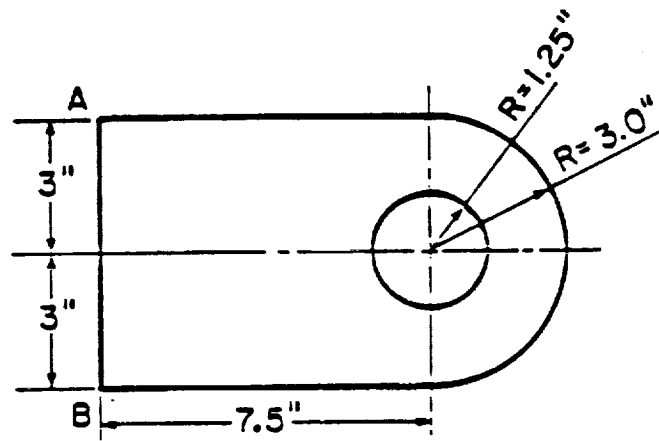
Figure 3.6 - Szabo's Model - Mesh 1
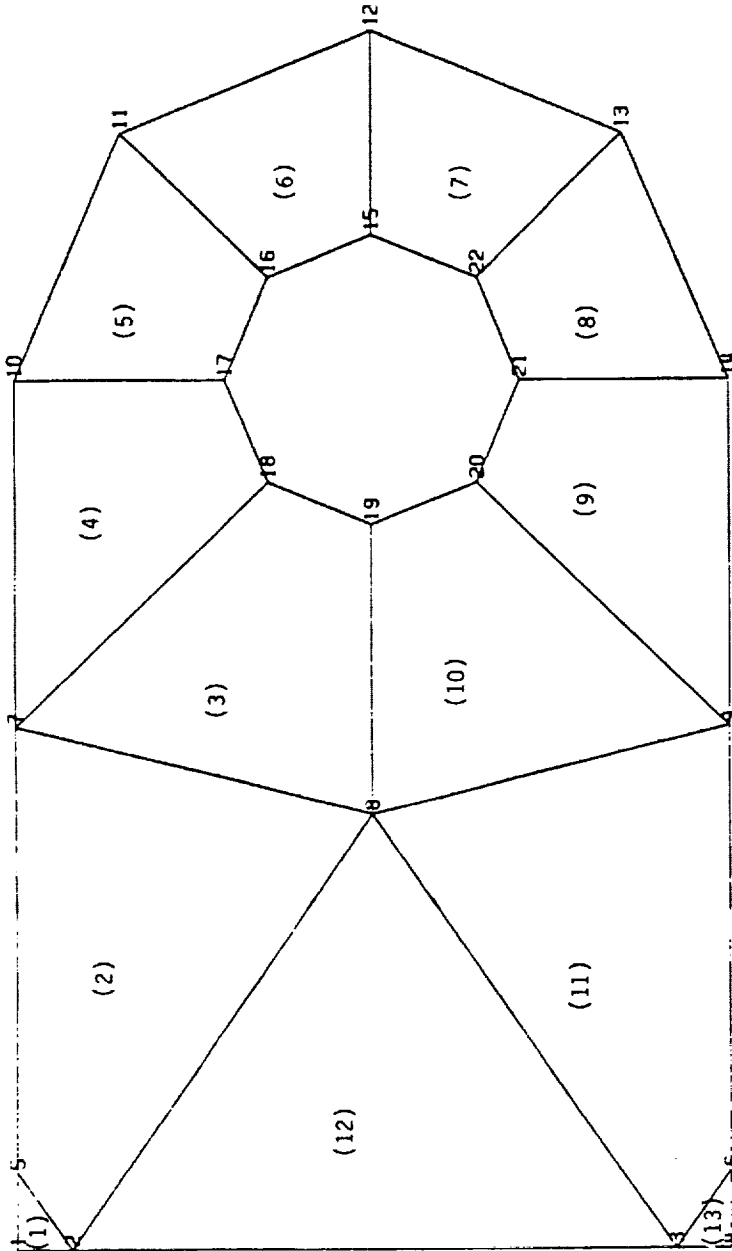
Figure 3.7 - Mesh 2 (Lug Problem)

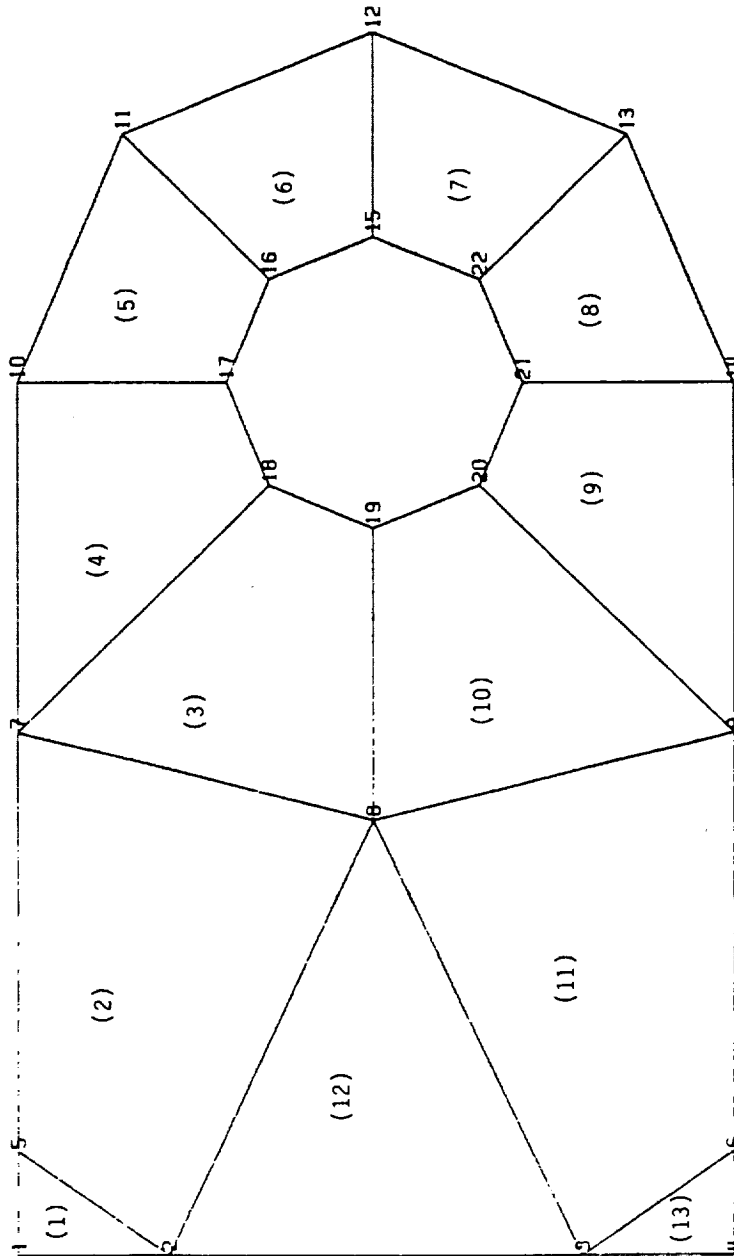Figure 3.8 - Mesh 3 (Lug Problem)

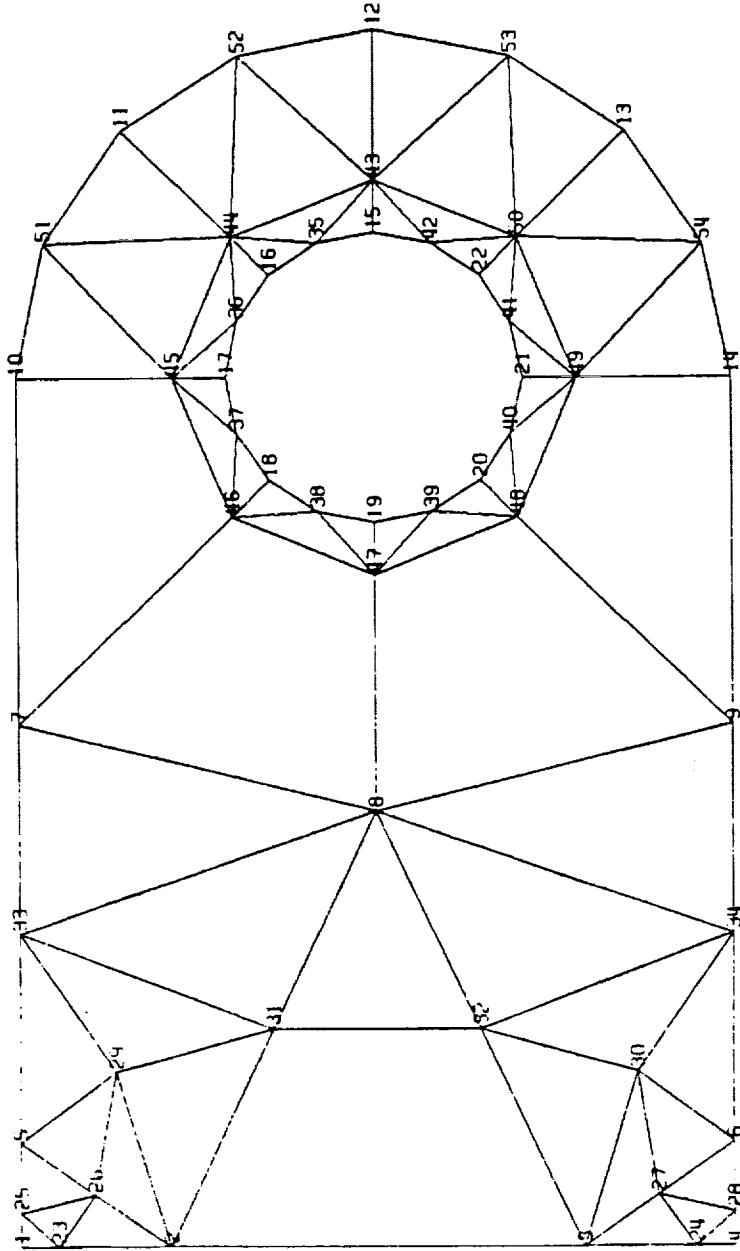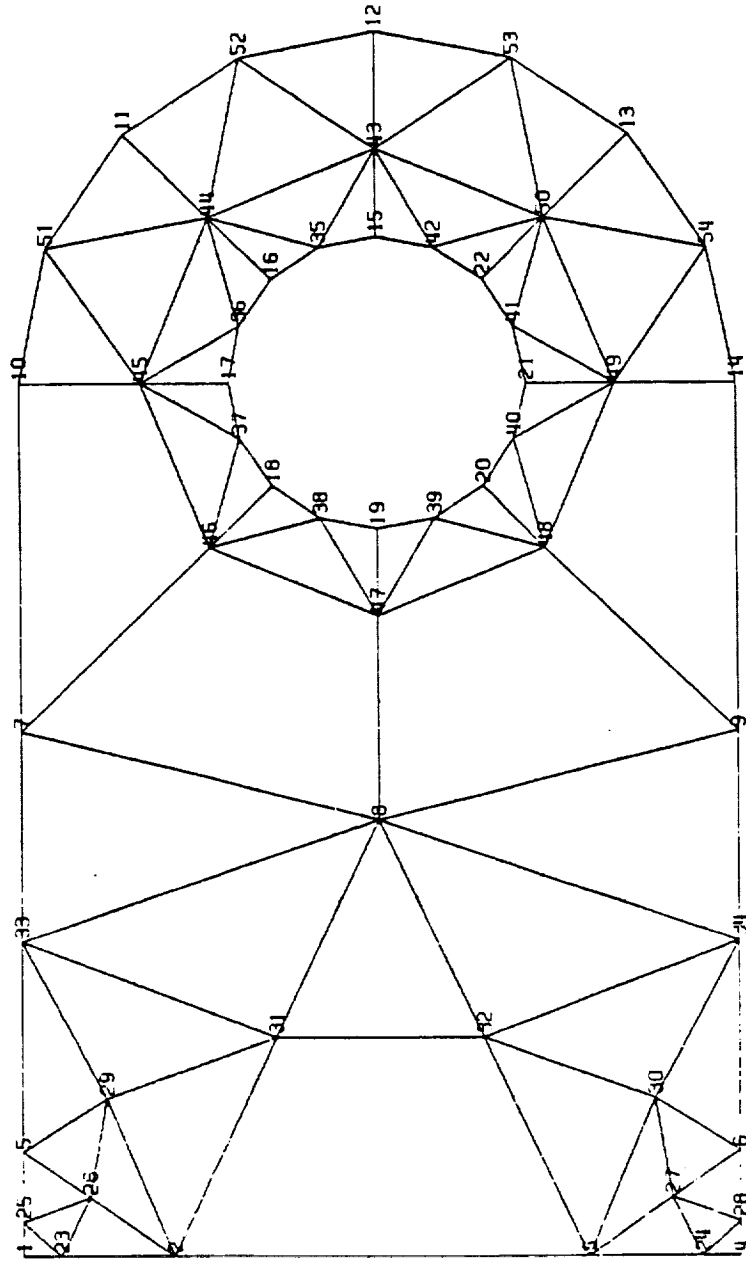**Figure 3.9 -** Mesh 4 (Lug Problem)

Figure 3.10 - Mesh 5 (Lug Problem)

3.4   DISK PROBLEM

3.4.1 DESCRIPTION

A disk with a uniform thickness of 0.5 inch and a 20 inch diameter is supported at two points B and C on its perimeter. It is loaded at a point A, on the perimeter as shown in Figure 3.11. It is modelled using TRIA6 elements of MSC-NASTRAN.

As indicated in the previous analysis of the lug, the initial mesh design is an important step in the analysis. The circular disk is axisymmetric. If the loads are also axisymmetric, then it is advantageous to maintain that symmetry by choosing annular ring elements. If the disk is modelled as shown in Figure 3.12, then symmetry about four planes is retained. However, the boundary conditions and the load warrant only symmetry about one plane passing through AD. In this study, the interior nodes are located on the circumference of a circle. Let r_m be the radius of this circle. The non-dimensional parameter $\xi = r_m/r_o$ is varied to change the mesh design.

The graph in Figure 3.13 shows the variation of the trace of the

global stiffness matrix and displacement at the center and Figure 3.14 shows the strain energy and displacement under the load as a function of ξ. The trace reaches its lowest value at $\xi = \xi_t = 0.53$. At values of ξ significantly different from ξ_t, elements become distorted leading to an increase in the trace. As grid points are moved towards the point of application of the load and support, the modeling of the region close to the periphery improves. This is indicated by the increase in the values of displacement under the load and strain energy. However, the improvement is restricted by the increasing distortion of the elements which is indicated by the increase in trace values. Therefore, both displacement under the load and strain energy reach their maximum values at $\xi = \xi_r$. They then decrease in a similar fashion. It is evident that ξ_t and ξ_r do not coincide. The point at the center of the disk is farthest from the periphery, and therefore, in accordance with the theory of Saint - Venant, it should be least affected by the load and the boundary conditions imposed. The displacement at the center reaches the maximum at ξ_t, the value at which the trace goes to a minimum. This shows that a minimum trace procedure yields a good mesh in the regions away from the boundaries and loads. However it is not the best mesh for the specific loads and boundary conditions applied. In order to achieve this, one has to use h and p methods of refinements in the areas close to the boundaries. If the

restriction that the interior nodes need to be on the circumference of a circle, is relaxed, then the trace minimization procedure would yield a mesh that has the least element distorsion. Best results could be obtained by iterating on refinement and improvement steps until the error is below the tolerance level.

3.4.2 CONCLUSION

This study shows that the trace minimization procedure improves the mesh in an overall sense. For any specific load and restraint set, other mesh refinement techniques need to be used.

Figure 3.11 - Circular Disk with Load and Supports.

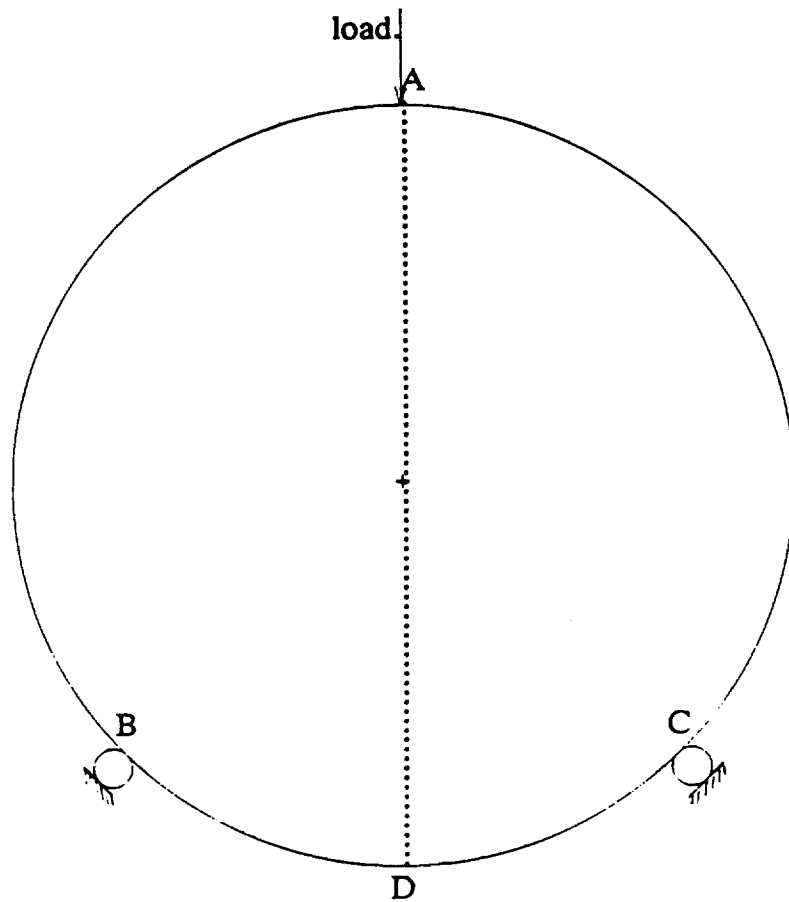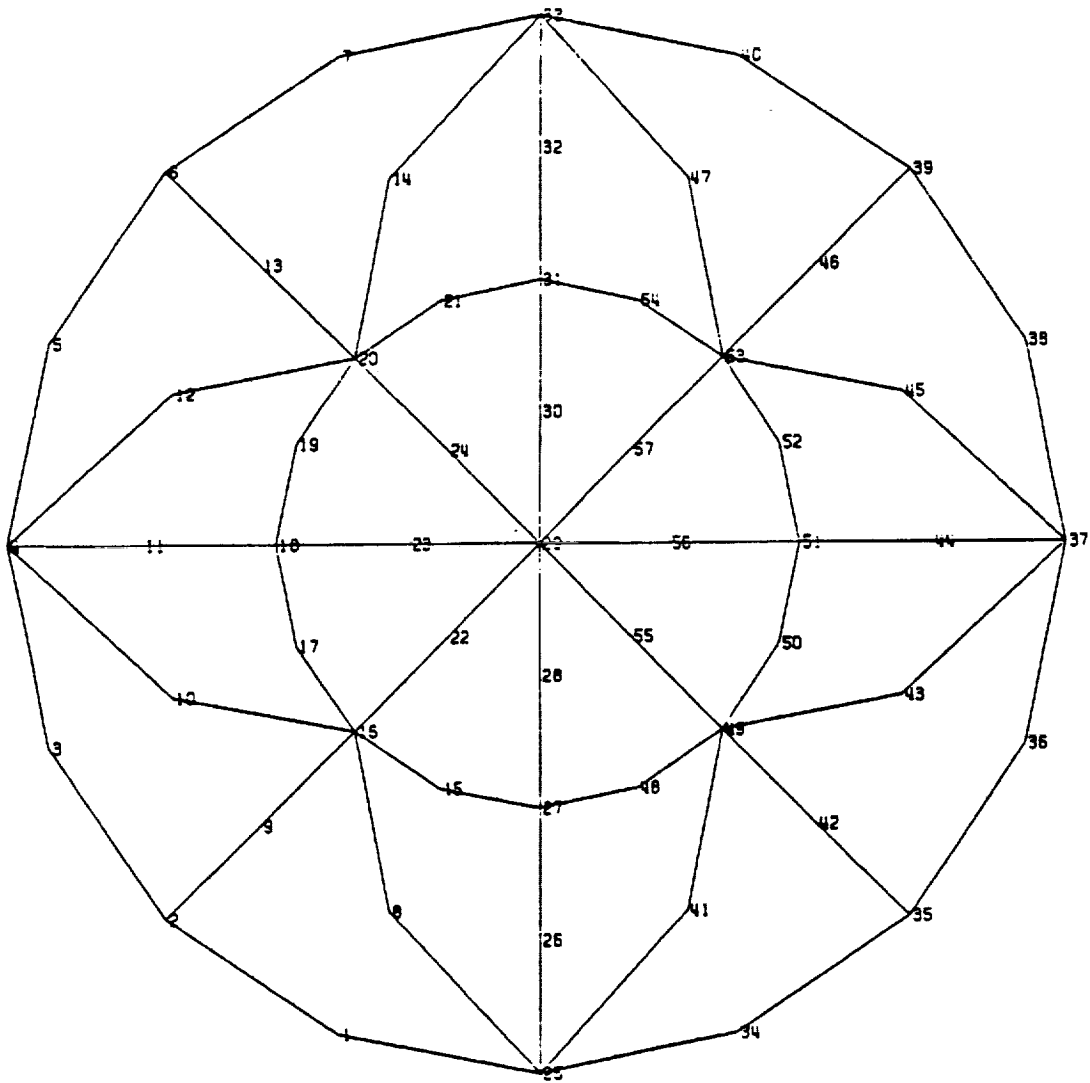Figure 3.12 - Disk Model Showing Four Fold Symmetry

68

Figure 3.13 - Graph of Trace and Displacement at the Center of the Disk
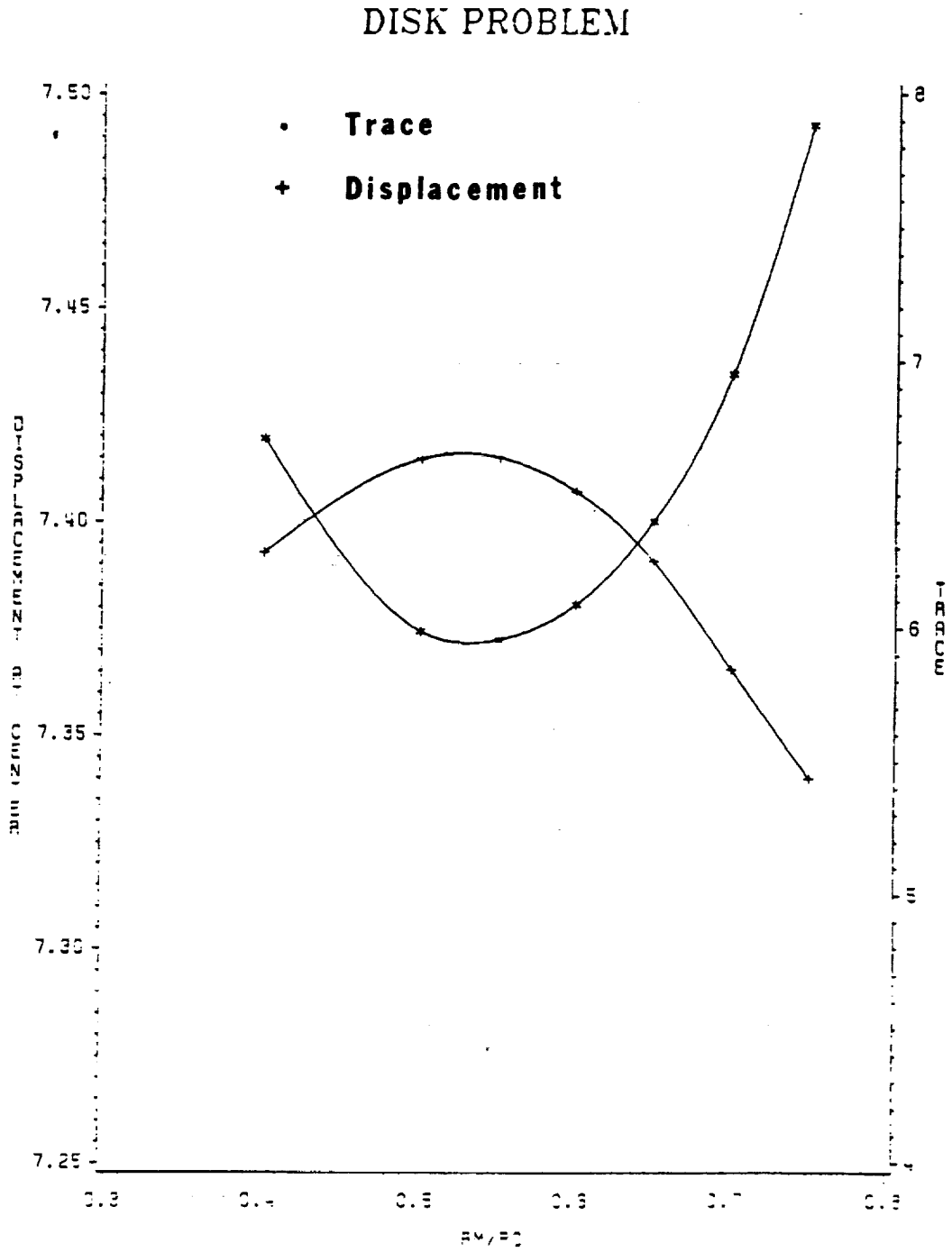
DISK PROBLEM

Figure 3.14 - Graph of Strain Energy and Displacement Under the Load on the Disk

DISK PROBLEM
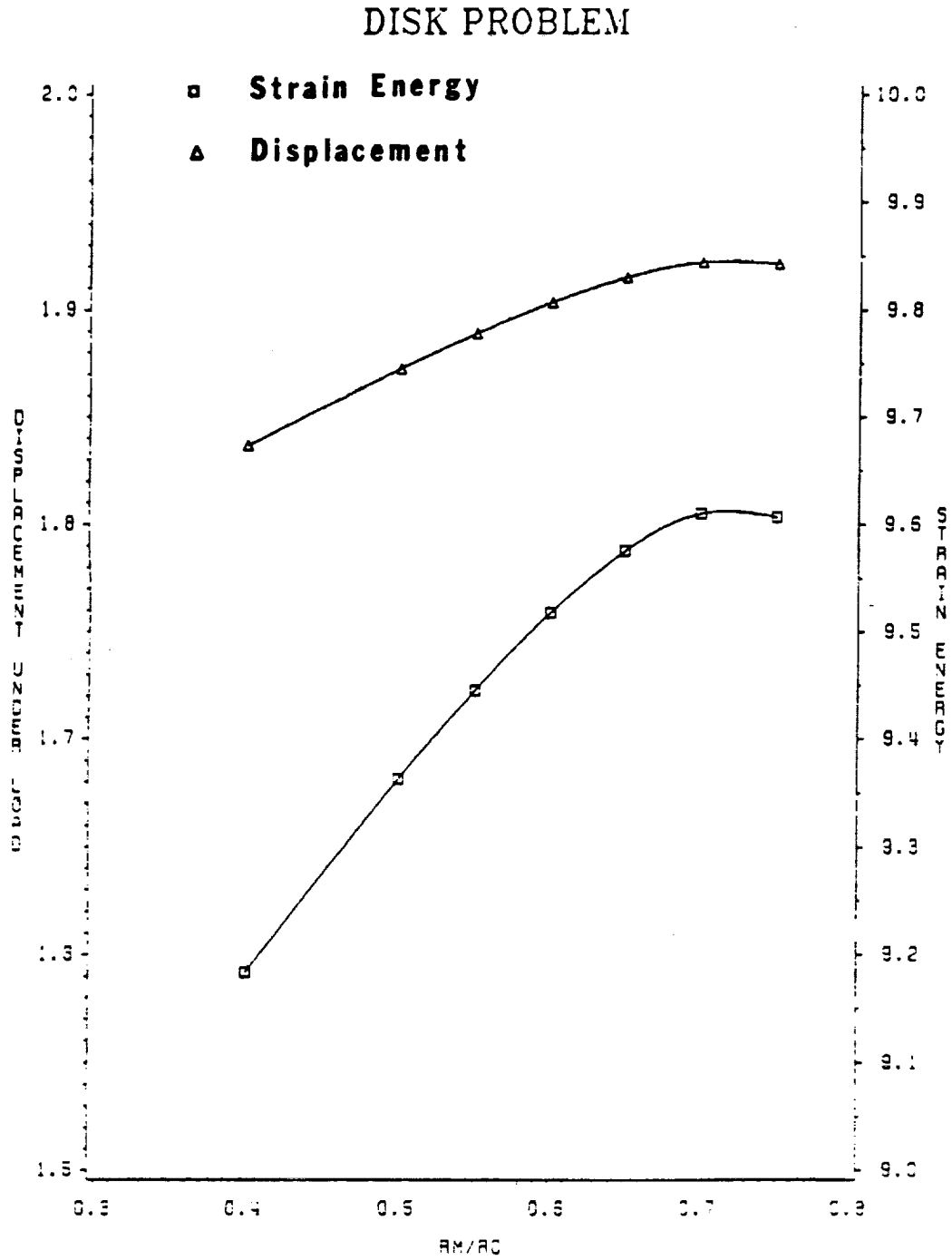
3.5 LAME PROBLEM

3.5.1 DESCRIPTION

One of the classic problems, used as a bench mark by most researchers, is that of a cylinder subjected to internal or external pressure. Lame provided the theoretical solution for an infinitely long cylinder. Lame's results can be used to evaluate the accuracy of finite element results. Since it is possible to have models of only finite length, there is an inherent error associated with the model. Moreover, when the cylinder is divided into elements, discretization errors are introduced. The focus of this study is on the minimization of discretization error by designing good grid patterns.

Consider a cylinder of inside radius $r_0 = 5$ cms, outside radius $r_a = 10$ cms, and length $L = 40$ cms as shown in Figure 3.15. Using symmetry of the cylinder, only one half of the cylinder is modelled with the nodes on the mid-section plane restrained in the axial direction. Two stacks of triangular ring elements of MSC-NASTRAN are used as shown in Figure 3.16. The nodes common to both stacks are arranged to be on a cylindrical surface of radius r_m. The non-dimensional parameter

$\xi = r_m/r_0$ is changed to vary the mesh pattern.

The graph in Figure 3.17 shows the variation of the trace of the global stiffness matrix and the variation of the strain energy with respect to ξ. Figure 3.18 shows that of the average radial displacement at the inside surface. The average radial displacement is computed by adding the radial displacement values at all the nodes on the inside surface and dividing the sum by the number of nodes. The trace reaches its maximum value at $\xi = \xi_t - 0.7072$ which is the geometric mean of the inside and the outside radii. The strain energy reaches its peak at $\xi = \xi_e$. It is seen that ξ_e is slightly smaller than ξ_t. For a uniform mesh $\xi = \xi_u = 0.745$. If strain energy is used as a criterion for convergence of the finite element solution, then the mesh with $\xi = \xi_e$ would provide the best mesh. However, the mesh with minimum trace is very close to the best mesh. Moreover it has been obtained without solving the equilibrium equations. The study shows that the minimum trace mesh is an improvement over the uniform mesh.

Convergence of strain energy does not guarantee the convergence of displacement and stress values [17]. The average radial displacement at the inside surface reaches its maximum at $\xi = \xi_d$, where ξ_d is smaller than ξ_e. Once again the mesh with minimum trace is an improvement over the

72

uniform mesh because ξ_t is closer to ξ_d than ξ_u.

3.5.2 CONCLUSION

The study confirms that the trace minimization procedure will provide a good starting mesh. Fewer refinement iterations will be needed to achieve convergence in the finite element solutions.

Figure 3.15 - Cylinder (Lame Problem)
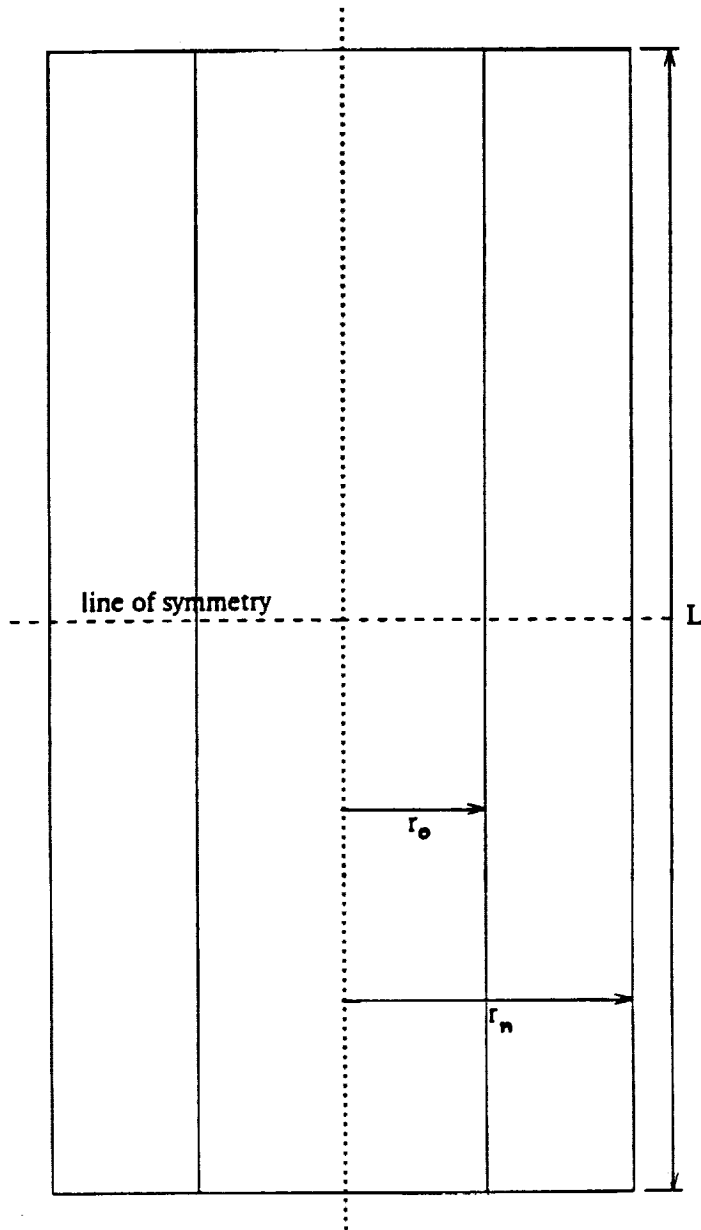
Figure 3.16 - Finite Element Model of the Cylinder (Lame Problem)
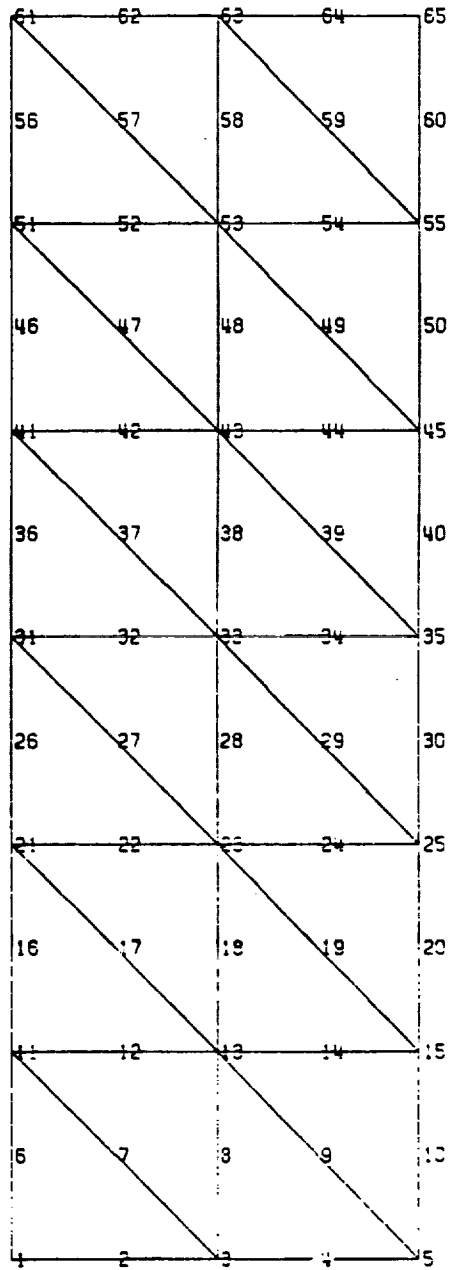
Figure 3.17 - Graph of Trace and Strain Energy (Lame Problem)
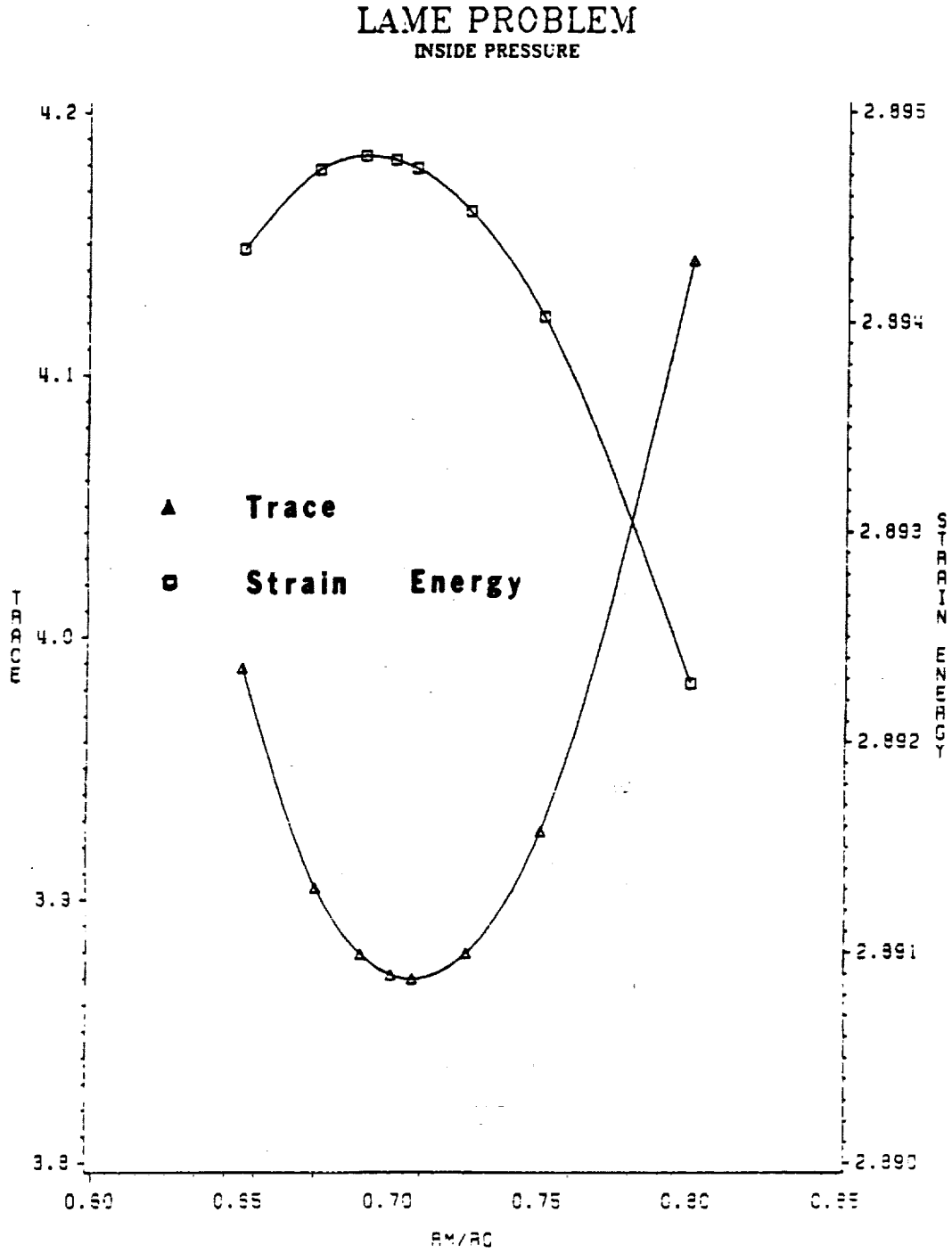
LAME PROBLEM
INSIDE PRESSURE

▲ Trace

▫ Strain Energy

Figure 3.18 - Graph of Average Radial Displacement at the Inside Surface (Lame Problem)

LAME PROBLEM
INSIDE PRESSURE
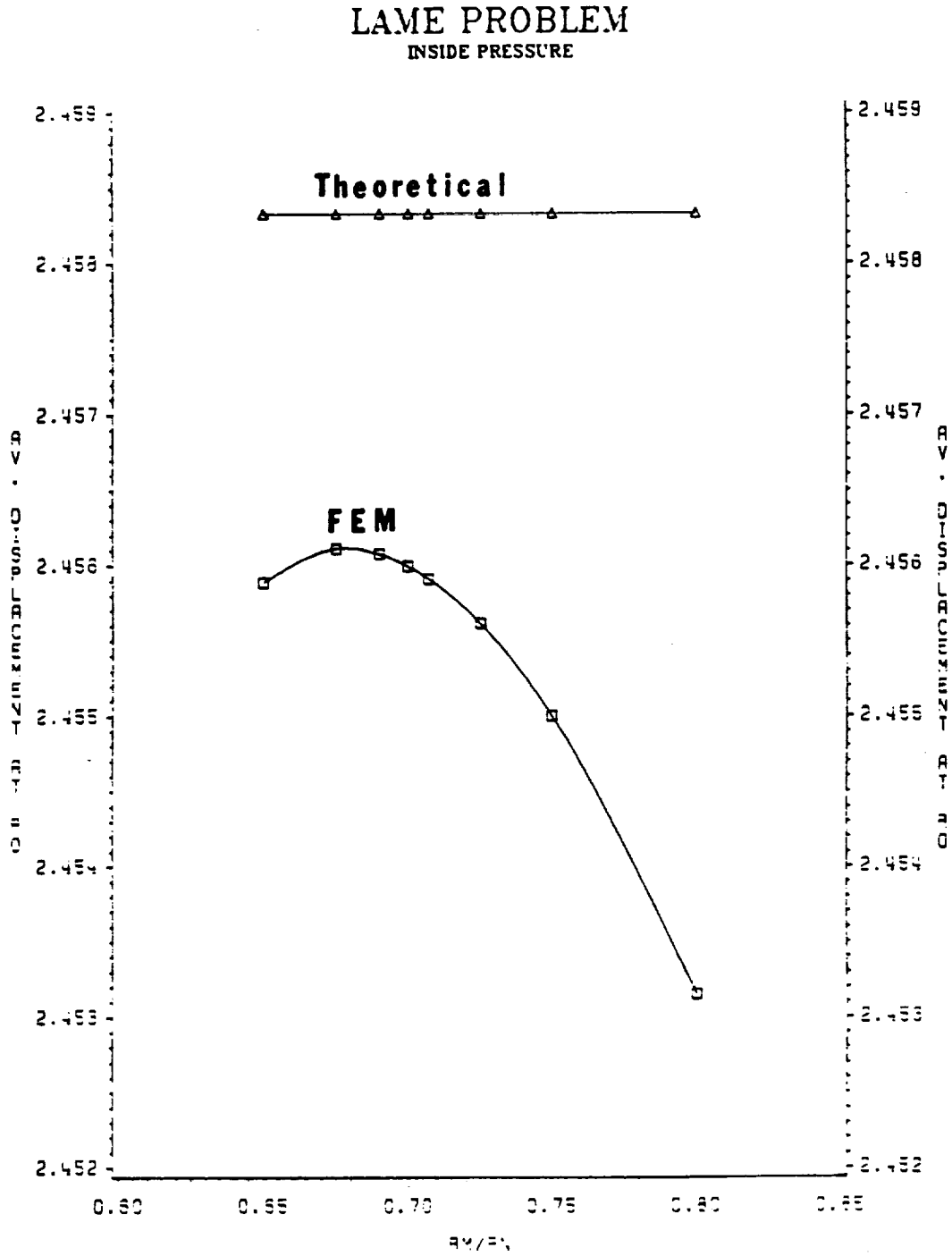
4. ALGORITHM DEVELOPMENT

The example problems have shown that the trace minimization procedure yields either an optimal mesh, as in the Prager problem, or a near optimal mesh as in the other examples. In either case it yields a very good starting mesh.

In any given problem, it may not be difficult to obtain an expression for the trace of the stiffness matrix. It would, however, be very difficult to obtain recursive relations by minimizing the trace of the matrix with respect to the nodal coordinates in order to obtain the grid configuration. Instead, let any arbitrary mesh (usually uniform mesh) be selected. This mesh may then be improved by relocating the nodes such that the value of the trace is lowered. The algorithm for trace minimization is shown in the flow chart in Figure 4.1.

There are three fundamental issues which are important for the success of the algorithm. First, the nodes that should be relocated need to be identified. Second, the direction and magnitude of the movement of each of the identified nodes need to be determined. Third, a criterion for the termination of the improvement iteration loop needs to be established.

78

The node identification step is relatively simple. Let k_{ll} and k_{ss} be the largest and the smallest diagonal entries on the stiffness matrix. Analogous to the methods of bisection, nodes associated with stiffness entries larger than $1/2 (k_{ll} + k_{ss})$ must be relocated. In general, the "cut-off" value could be expressed as $\eta_c (K_{ll} + K_{ss})$, where $\eta_c = 0.5$ is one specific choice. However, for best results, η_c could be determined by numerical experimentation.

Next, one or several nodes could be moved at a time. The latter choice of the two will certainly reduce the CPU time. Let ϕ_i be the set of elements connected to node "i". Let ψ_i be the set of nodes associated with elements in ϕ_i. Then the set ψ_i can be described as the "neighbor set of node i". Note that in FEM, relocation of node "i" will effect a change in the stiffness associated with its neighbor set only. One of the fundamental requirements for better control in the process is to be able to distinguish the effects of each individual change. Therefore two nodes, i and j, will qualify for relocation only if there are no common nodes in their neighbor sets ψ_i and ψ_j. In mathematical terms, the intersection of neighbor sets of all qualifying nodes should be an empty set.

The determination of the direction and magnitude of the movement of each identified nodes from its old location to its new location is

79

relatively difficult. Observe that in **the Prager** problem, the scalar coefficient in the determination of the trace (Equation 3.6) is given by $EA(x)/l(x)$. Any relocation of the node which increases the element length also decreases the cross sectional area. Therefore it reduces the stiffness contribution to the trace. Node relocations can be accomplished by observing the expressions for element stiffnesses and the role of each of the parameters involved such as $A(x)$ and $l(x)$ in the tapered bar problem. Each node can be selected and moved to a new location manually by using a graphic terminal. However the process is slow, cumbersome and inefficient.

Another approach is, for each identified node, to obtain its neighbor set. Then compute the trace of the submatrix corresponding to the neighbor set, and store it. The most important step in this approach is the determination of the trace gradient. In the one dimensional case, the gradient can be computed by difference formulae once the value of the trace is known at another point. Therefore, select a new location at some distance away. (A discussion on the magnitude of this distance is given in the following paragraph). Next, compute the trace of the neighbor set corresponding to the new location. The trace gradient computed will indicate the direction and magnitude of movement for relocation. In the two dimensional case, first compute the trace of the submatrix

corresponding to the neighbor set of the node in its original location as described before. Second, select a new location for the node in any direction and compute the trace. Next, select another location in a direction perpendicular to the direction chosen for the selection of the first new location. Again compute the trace. Using the three trace values, gradients in the two mutually perpendicular direction can be computed, which when added vectorially will yield the gradient at the original location. Similarly, in the three dimensional case, three new locations on three mutually perpendicular lines should be used. Finally, the node should be moved in the direction indicated by the gradient.

The magnitude of movement for gradient computation and for final node relocation will be a fixed percentage of the distance between the node under consideration and its neighbor in the direction of the gradient. However the percentage can be fixed empirically and/or by numerical experimentation.

The objective of this algorithm is to produce a mesh with the least trace value. The hypothesis is that the trace minimization procedure will distribute the stiffness uniformly among the nodes and elements. Therefore the criterion for termination of the improvement iteration loop can be based either directly on the decrement in trace value or the uniformity of

the stiffness values at all node points.

To see how uniform stiffness results in a uniform distribution of error and therefore yields the best mesh, consider a finite element model with n degrees of freedom (d.o.f.). If the mesh is to be refined by introducing additional nodes, then it is necessary to know the expected improvement in error before a refinement step is undertaken. O.C. Zienkiewicz et. al. [20] and Peano et. al. [21] have shown that if the $n+1^{th}$ d.o.f. is to be introduced hierarchically, then the error in the energy norm is:

$$(4.1) \qquad \left\| e_{n,1} \right\|^2 = \frac{(f_{n+1} - K_{n+1,n}u_n)^2}{K_{n+1,n+1}}$$

where, f_{n+1} is force corresponding to the $n+1^{th}$ d.o.f., $K_{n+1,n+1}$ is the stiffness of the $n+1^{th}$ d.o.f., $K_{n+1,n}$ is the off-diagonal stiffness relating the $n+1^{th}$ d.o.f. to the original n d.o.f. system, and u_n is the array of nodal displacements of the n d.o.f. system. The subscripts n,1 of the error e refer to the n original d.o.f. and the new d.o.f.

Zienkiewicz [22] has used the above error relation to define an error indicator in the form:

$$(4.2) \qquad \eta_{n,1}^2 = \frac{\left(\int_\Omega \varsigma \, N_{n+1} \, d\Omega \right)^2}{K_{n+1,n+1}}$$

where, ς is the finite element residual.

In an adaptive refinement strategy, these indicators are normally calculated for all the d.o.f. corresponding to the **next** refinement. The indicators serve the purpose of identifying the region where refinement is necessary.

Next, the error corresponding to the previous iteration wherein the nth d.o.f. was added, is:

$$(4.3) \qquad \left\| \, e_{n-1,1} \, \right\|^2 = \frac{(\, f_n - K_{n,n-1} u_{n-1} \,)^2}{K_{n,n}}$$

The corresponding error indicator is:

$$(4.4) \qquad \eta_{n-1,1}^2 = \frac{\left(\int_\Omega \varsigma \, N_n \, d\Omega \right)^2}{K_{n,n}}$$

These derivations are for the hierarchical finite elements. However, the error with the conventional finite elements will be of a similar form.

The most general method of generating good grids is to have an equal distribution of some specified weight function. (See Eiseman [23] for a complete discussion on adaptive grid generation.) Often, the error in the finite element solution is used as the weight function [24]. Therefore the objective is to distribute the error equally among all elements. However, the value of the residual ς can be obtained only after the equilibrium equations are solved. Nevertheless, one way of obtaining an equi-distribution of error a priori is by having uniform element stiffnesses. As a consequence, ς will be nearly uniform among the elements. The trace minimization procedure developed herein produces such a result.

Consider again the Heat Transfer Example of section 3.2. Note that each of the ratios in the optimality condition, Equation (3.44), can be equated to a constant γ.

$$(4.5) \qquad \frac{r_1}{r_0} = \frac{r_2}{r_1} = \cdots = \frac{r_{e+1}}{r_e} = \cdots = \frac{r_n}{r_{n-1}} = \gamma$$

Substituting into Equation (3.42), the element stiffness coefficient is :

$$(4.6) \qquad S_e = \pi \, k_e \, \frac{\gamma + 1}{\gamma - 1}$$

which is a constant. Therefore the trace minimization procedure

produces a uniform element stiffness.

Finally, observe the graphs of errors in Figures 4.2, 4.3 and 4.4. The errors are equally distributed with the improved mesh. There is a skewed distribution with the uniform mesh. In order to compare the error distribution among the elements, rms errors were calculated using 50 uniformly spaced points along the length of each element. Also the overall rms error for the model was calculated using all the points. Table 4.1 shows the rms error distribution. Note that in all the cases, the improved mesh distributes the error more uniformly than the uniform mesh. The rms errors on the elements are almost exactly equal in the case where temperatures are specified at the boundaries. Therefore the mesh obtained is optimal. Similar results, however, are not obtained in the case where both temperature and temperature gradient are specified because of the inability of FEM to strongly satisfy the Neumann boundary conditions [25]. Nevertheless, it demonstrates the usefulness of the trace minimization procedure in a priori grid refinement.

TABLE 4.1 - Comparison of RMS Error Distribution Among the Elements Between Finite Element Uniform Mesh and Improved Mesh for the Two Models with Different Boundary Conditions.

| | Temperature B.C. | | Temperature/Gradient B.C. | | | |
| | Temperature | | Temperature | | Gradient | |
	Uniform	Improved	Uniform	Improved	Uniform	Improved
Element 1	1.0479	0.5171	0.6786	0.2402	0.6029	0.5183
Element 2	0.6688	0.5171	0.4237	0.2980	0.3594	0.4122
Element 3	0.4422	0.5171	0.3082	0.3782	0.2392	0.3278
Element 4	0.2857	0.5171	0.2430	0.4694	0.1134	0.1654
Overall	0.6800	0.5210	0.4494	0.3586	0.3755	0.3781

Another advantage of using uniform stiffness criterion is that the matrix condition number improves. Matrix condition number κ may be shown that:

$$(4.7) \qquad \kappa = \frac{\lambda_{max}}{\lambda_{min}}$$

where λ_{max} is the largest and λ_{min} is the smallest eigen values of matrix K. When, definition (4.7) is used, κ it is called the spectral condition number. If k_s and k_{11} denote the smallest and largest diagonal entry of matrix K, an expression for the lower bound for κ would be:

$$(4.8) \qquad \kappa \geq \frac{k_{11}}{k_s}$$

Utku and Melosh [27] have shown that the decimal digits lost in computation of displacements in finite elements to be:

$$(4.9) \quad D = p + \log_{10} e_q + \log_{10} \kappa$$

where D is the decimal digits lost in the computation, e_q is the residual unbalanced error and p is the precision of the machine in decimal digits. Note that for a mesh with uniform stiffnesses, $k_{11} \approx k_{nn}$ and therefore $k \geq 1$. If K is equal to unity, then digits lost in the computation is the minimum. The criterion of uniform stiffness therefore attempts to obtain results with the least manipulation error.

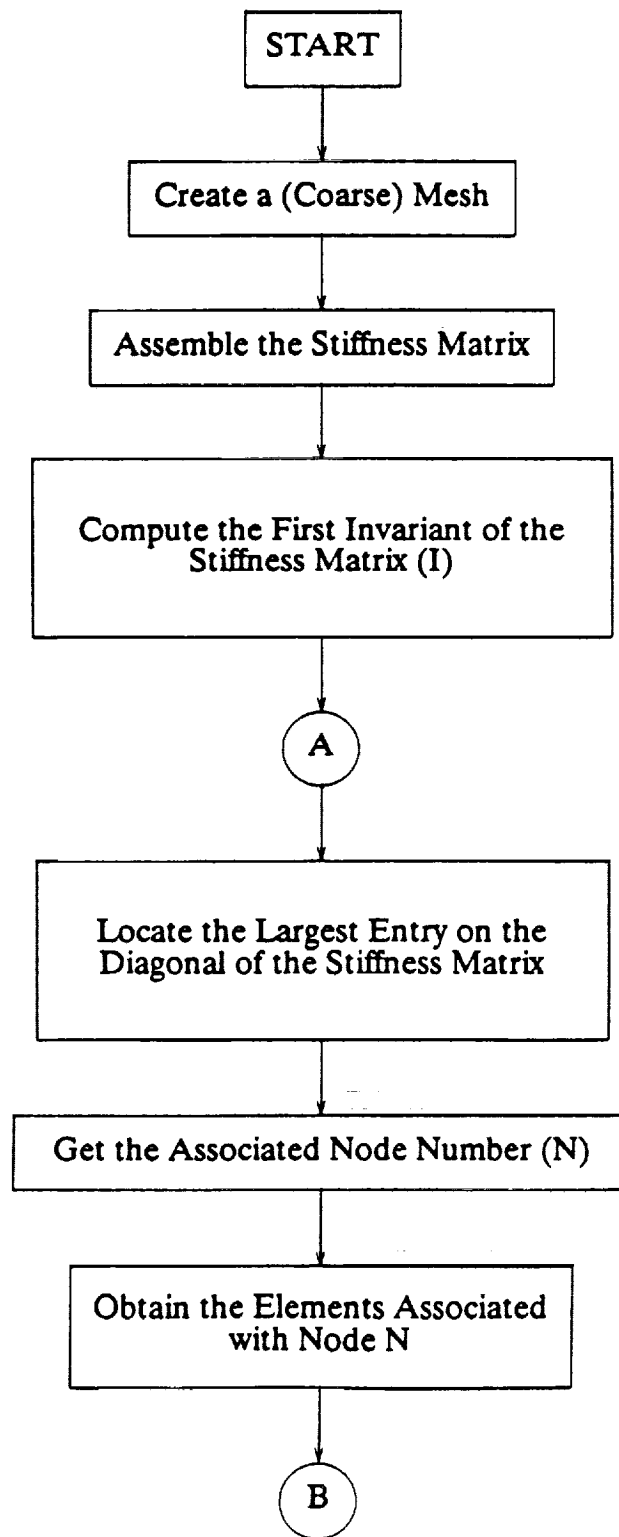**Figure 4.1 -** Flow Chart of Trace Minimization Algorithm

```
                    ┌─────────────┐
                    │    START    │
                    └─────────────┘
                           │
                           ▼
              ┌──────────────────────┐
              │ Create a (Coarse) Mesh │
              └──────────────────────┘
                           │
                           ▼
              ┌──────────────────────────┐
              │ Assemble the Stiffness Matrix │
              └──────────────────────────┘
                           │
                           ▼
          ┌──────────────────────────────────┐
          │  Compute the First Invariant of the │
          │        Stiffness Matrix (I)         │
          └──────────────────────────────────┘
                           │
                           ▼
                         ( A )
                           │
                           ▼
          ┌──────────────────────────────────┐
          │   Locate the Largest Entry on the   │
          │   Diagonal of the Stiffness Matrix  │
          └──────────────────────────────────┘
                           │
                           ▼
          ┌──────────────────────────────────┐
          │  Get the Associated Node Number (N) │
          └──────────────────────────────────┘
                           │
                           ▼
          ┌──────────────────────────────────┐
          │   Obtain the Elements Associated    │
          │            with Node N              │
          └──────────────────────────────────┘
                           │
                           ▼
                         ( B )
```
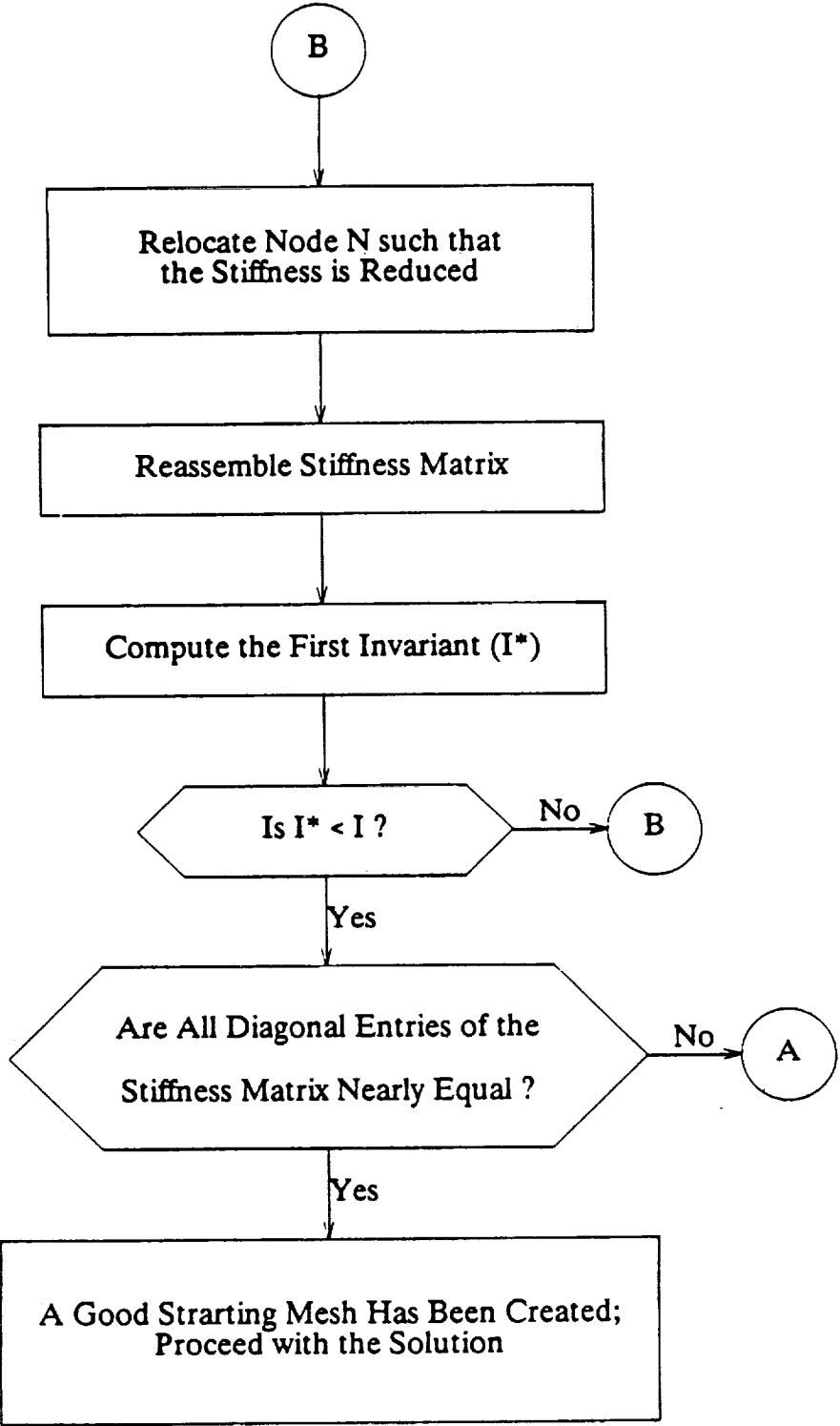
88

Figure 4.1 (cont)

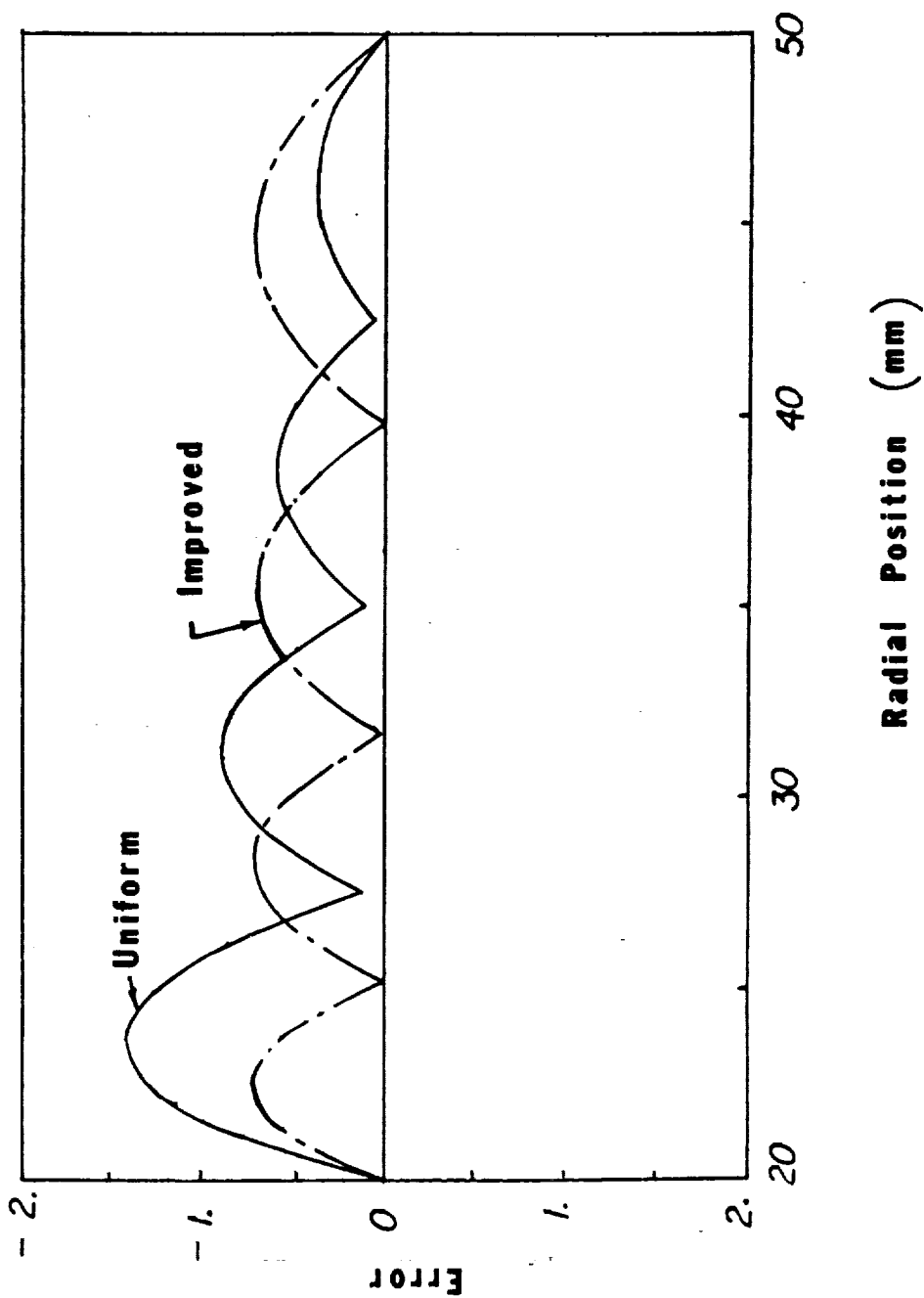**Figure 4.2** - Graph of Error in Temperature in the Cylinder Model with Temperature Specified Boundary Conditions

Figure 4.3 - Graph of Error in Temperature in the Cylinder Model with both Temperature and Temperature Gradient Specified Boundary Conditions
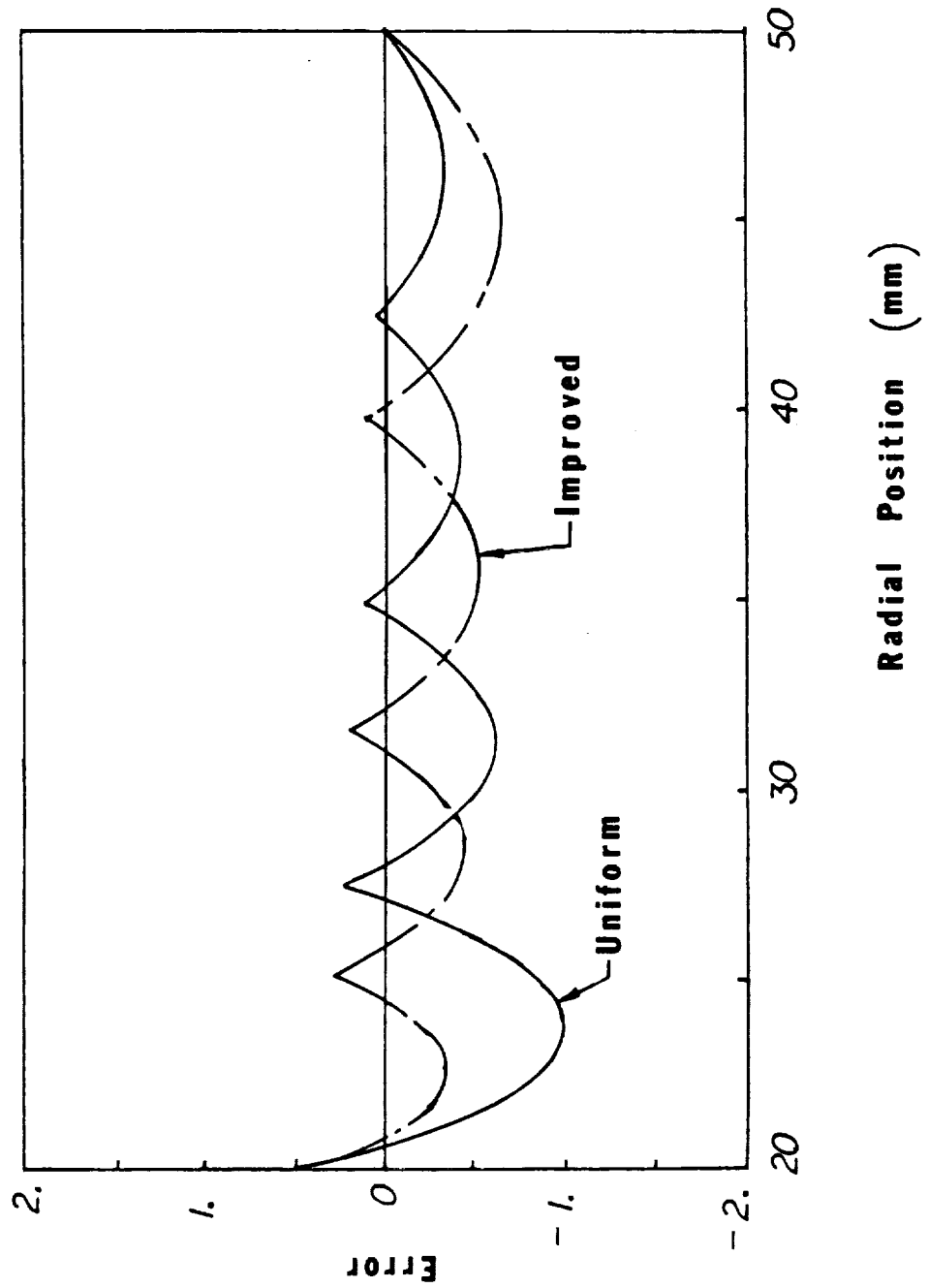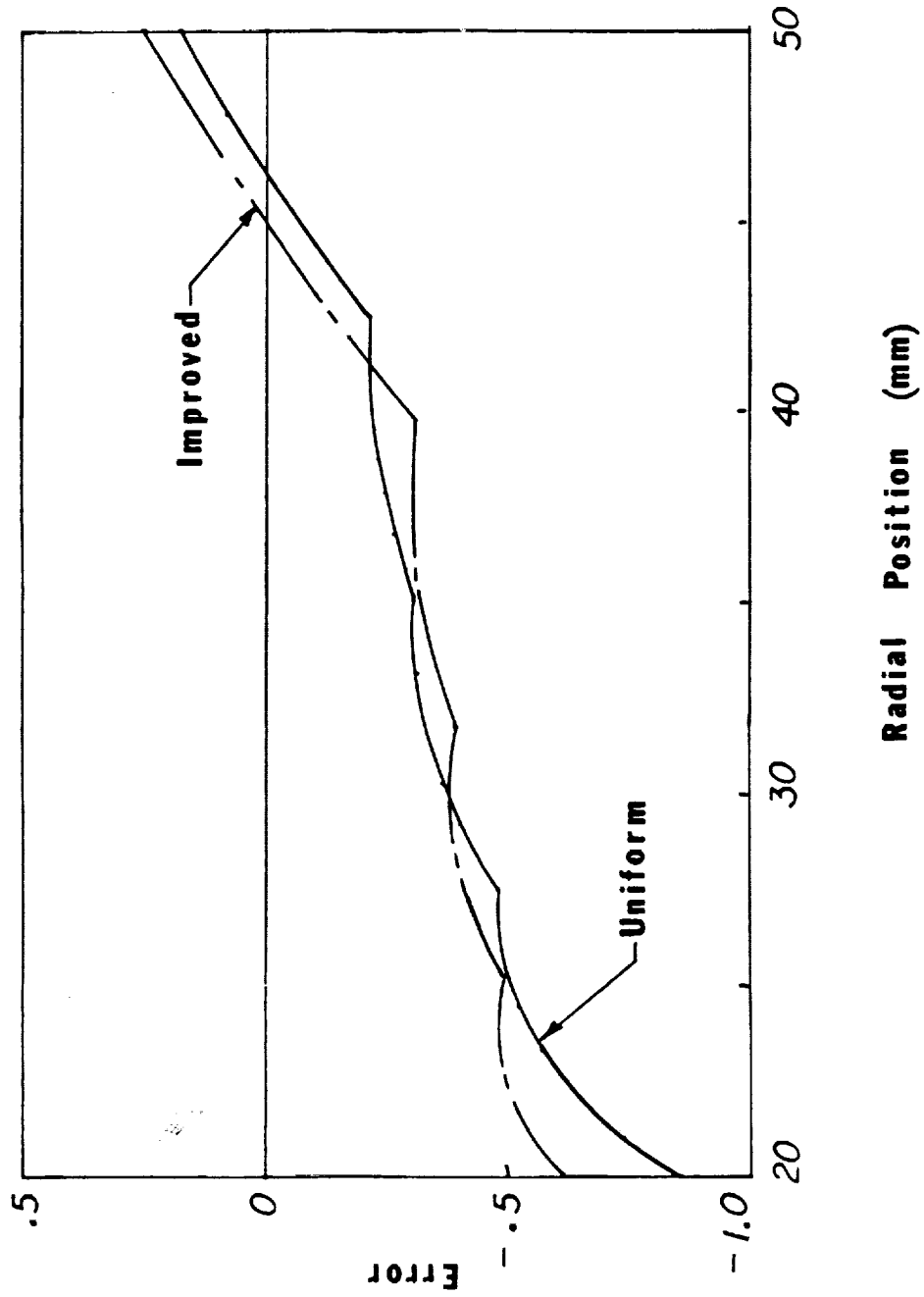
91

Figure 4.4 - Graph of Error in Temperature Gradients in the Cylinder model with both Temperature and Temperature Gradient Specified Boundary Conditions

5. CONCLUSIONS AND RECOMMENDATION

5.1 CONCLUSIONS

Making a proper choice of mesh is an important step in the finite element analysis for obtaining accurate results. Although engineering judgment and prior knowledge of analysis prove helpful in mesh design, the procedure of trace minimization makes it possible to obtain good meshes without depending upon such judgments and knowledge. Any arbitrary mesh may be used. The procedure then relocates the nodes such that the value of the stiffness matrix trace is lowered. As a consequence it redistributes the total error nearly uniformly among the elements. Thus the resulting mesh is either optimal or near optimal. The main advantage of the procedure is that a good mesh can be obtained before the equilibrium equations are solved. A posteriori methods could be used to refine the mesh even further. With the use of the trace minimization procedure, fewer a posteriori refinements become necessary to obtain the desired accuracy level than when the procedure is not used.

Most finite element packages have routines to check the correctness of the mesh generated. They check node coincidences, element coincidence

$C - 2$

and element distortions. The routines iterate on the elements to check if the distortion is lower or higher than a set tolerance. As demonstrated in the aircraft lug analysis example, the trace minimization procedure yields a mesh with minimum element distortion - a useful byproduct. Moreover, if the algorithm presented in Chapter 4 is implemented properly, the CPU time required may not be excessively larger than that required for the routines used for a distortion check.

Finally, the procedure improves the stiffness matrix condition number and therefore reduces the truncation errors. The benefits derived obviously outweigh the cost of implementing the procedure.

5.2 RECOMMENDATIONS

The algorithm outlined in Chapter 4 needs to be coded for efficient processing. Some of the constants, such as the cut off parameter, need to be determined by numerical experimentations. The procedure needs to be validated by applying it with problems belonging to classes other than those considered in this dissertation work.

In most structural problems, the stiffness matrix is symmetric and

positive definite. The procedure developed is based upon these assumptions. It will be useful to develop similar procedures for problems with stiffness matrices that are non-symmetric and not positive definite.

6. REFERENCES

[1]   Zienkiewicz, O. C.: *The Finite Element Method*; 3rd edition, McGraw Hill, New York, 1977.

[2]   Zienkiewicz, O. C., Morgan, K.: *Finite Elements and Approximation*, John Wiley & Sons, New York, 1983.

[3]   Segerlind, L. J.: *Applied Finite Element Analysis*, Wiley, New York, 1984.

[4]   Reddy, J. N.: *Energy and Variational Methods in Applied Mechanics: With an Introduction to the Finite Element Method*, Wiley, New York, 1984.

[5]   Huston, R. L. and Passerello, C. E.: *Finite Element Method: An Introduction*, M. Dekker, New York, 1984.

[6]   Shephard, M. S.: "Approaches to the Automatic Generation and Control of Finite Element Meshes", Applied Mechanics Review, Vol. 41, No. 4, April 1988.

[7]   Brown, P. R.: "A Non-Interactive Method for the Automatic Generation of Finite Element Meshes Using the Schwarz-Christoffel

Transformations", Computer Methods in Applied Mechanics and Engineering, 25 (1981), 101-126.

[8]   Shephard, M. S.: "Finite Element Grid Optimization with Interactive Computer Graphics", Ph.D. Dissertation, Cornell University, January 1979.

[9]   Prager, W.: "A Note on the Optimal Choice of Finite Element Grids", Comp. Methods Appl. Mech. Eng., Vol. 6, No. 3, November 1975, pp. 363-366.

[10]   Melosh, R. J.: "Development of the Stiffness Method to Define Bounds on Elastic Behavior of Structures", Ph.D. Thesis, University of Washington, Seattle (1962).

[11]   Key, S. W.: "A Convergence Investigation of the Direct Stiffness Method", Ph.D. Thesis, University of Washington, Seattle (1966).

[12]   Carroll, W. E. and Barker, R. M.: "A Theorem for Optimum Finite Element Idealizations", Int. Journal of Solids & Structures, Vol. 9, (1973), 883-895.

[13]   Prenter, P. M.: *Splines and Variational Methods*, Pure and Applied Mathematics, Wiley-Interscience Series of Texts, John Wiley & Sons, New

York, 1975.

[14]   Robinson, J.: "An Introduction to Hierarchical Displacement Elements and the Adaptive Technique", Finite Elements in Analysis and Design, Vol. 2 (1986), 377-388.

[15]   Kittur, M. G.:   "Finite Element Mesh Improvement by the Minimization of the Stiffness Matrix Trace", Ph.D. Dissertation, University of Cincinnati, 1988.

[16]   Masur, E. F.:   "Some Remarks on the Optimal Choice of Finite Element Grids", Comp. Methods Appl. Mech. Eng., Vol. 14, May 1978, pp. 237-248.

[17]   Szabo, B. A.:   "Implementation of Finite Element Software System with h & p Extension Capabilities", Finite Elements in Analysis and Design 2 (1986), 177-194.

[18]   Babuska, I., Gui, W., and Szabo, B. A.: "Performance of the h, p and h - p versions of the Finite Element Method", Institute for Physical Science and Technology, Laboratory for Numerical Analysis, Technical Note BN - 1027 (September 1984).

[19]   Szabo, B. A.:   "Estimation and Control of Error Based on p - Convergence", Proc. Int. Conf. on Accuracy Estimates and Adaptive Refinements in Finite Element Computations (ARFEC), Lisbon, Portugal (1984).

[20]   Reed, K. W. and Cardinal, J. W.: "Finite Strain Analysis by a Stress-Function Method", Computational Mechanics, Vol. 2 (1987) 31-44.

[21]   Zienkiewicz, O. C. and Craig, A.:   "Adaptive Refinement, Error Estimates, Multigrid Solution, and Hierarchic Finite Element Method Concepts", Accuracy Estimates and Adaptive Refinements in Finite Element Computations, edited by Babuska, I., et. al., John Wiley & Sons Ltd., (1986).

[22]   Peano, A., Favelli, M., Riccioni, R., and Sardella, L.: "Self Adaptive Convergence at the Crack Tip of a Dam Buttress", Int. Conf. on Fracture Mechanics, Swansea (1979).

[23]   Zienkiewicz, O. C., Kelly, D. W., Gago, J. P. de S. R., and Babuska, I.: "Hierarchical Finite Element Approaches, Adaptive Refinements and Error Estimates", The Mathematics of Finite Elements and Applications, Editor Whiteman, J. R., Academic Press (1982).

[24]   Eiseman, P. R.: "Adaptive Grid Generation", Computer Methods in

Applied Mechanics and Engineering, Vol. 64, Nos. 1-3, October 1987, pp. 321-376.

[25]   Gago, J. P. de S. R., Kelly, D. W., and Zienkiewicz, O. C., "A Posteriori Error Analysis and Adaptive Processes in the Finite Element Method: Part II - Adaptive Mesh Refinement", Int. J. for Num. Methods in Engineering, Vol. 19, pp. 1621-1656.

[26]   Thomasset, F.: *Implementation of Finite Element Methods for Navier-Stokes Equations*, Springer Series in Computational Physics, 1981, pp. 11.

[27]   Fried, I. and Yang, S. K., "Best Finite Element Distribution Around a Singularity", AIAA Journal, Vol. 10, September (1972), pp. 1244-1246.

[28]   Fried, I.: "Discretization and Round-Off Errors in the Finite Element Analysis of Elliptic Boundary Value Problems and Eigenvalue Problems", Ph.D. Dissertation, MIT, 1971.

APPENDIX

MSC-NASTRAN allows the user to compute intermediate values or custom build solution sequences via the Direct Matrix Abstraction Program known as DMAP module. These DMAP instructions typically preceed the last card "CEND" in the Executive Control Deck. The following set of DMAP instructions were used in the trace calculations:

Nastran Executive Control Deck

```
ID   PROBLEM3,LUG

TIME  1

SOL  24

•

ALTER  219

DIAGONAL  KGG/KGGD/     $

MATGEN  ,  /IDEN/1/NDF/0/0  $

DIAGONAL  IDEN/IVEC/  $

TRNSP  IVEC/IVECT/  $

SMPYAD  IVECT,KGGD,,,,/TRACE/2/////////2  $

MATPRN  TRACE  //  $

CEND
```

Case Control Deck.

Where KGG is the global stiffness matrix, KGGD is the vector of diagonal stiffness entries, IDEN is an identity matrix of size NDF by NDF, IVEC is the vector of diagonal entries of IDEN, IVECT is transpose of IVEC and TRACE is a matrix of size 1 by 1 and contains the value of the trace. Note that in the instruction for matrix generation the variable NDF has to be replaced by the number of degrees of freedom in the model.

Report Documentation Page

1. Report No. NASA CR-185170 AVSCOM TR 89-C-019	2. Government Accession No.	3. Recipient's Catalog No.
4. Title and Subtitle Mesh Refinement in Finite Element Analysis by Minimization of the Stiffness Matrix Trace		5. Report Date November 1989
		6. Performing Organization Code
7. Author(s) Madan G. Kittur and Ronald L. Huston		8. Performing Organization Report No. None
		10. Work Unit No. 1L162209A47A 505-63-51
9. Performing Organization Name and Address University of Cincinnati Department of Mechanical and Industrial Engineering Cincinnati, Ohio 45221-0072		11. Contract or Grant No. NSG-3188
12. Sponsoring Agency Name and Address Propulsion Directorate U.S. Army Aviation Research and Technology Activity—AVSCOM Cleveland, Ohio 44135-3127 and NASA Lewis Research Center Cleveland, Ohio 44135-3191		13. Type of Report and Period Covered Contractor Report Final
		14. Sponsoring Agency Code

15. Supplementary Notes

Project Manager, Fred B. Oswald, Propulsion Systems Division, NASA Lewis Research Center. Madan G. Kittur, presently employed by Aero Structures, Arlington, Virginia. Ronald L. Huston, University of Cincinnati.

16. Abstract

Most Finite Element packages provide means to generate meshes automatically. However, the user is usually confronted with the problem of not knowing whether the mesh generated is appropriate for the problem at hand. Since the accuracy of the Finite Element results is mesh dependent, mesh selection forms a very important step in the analysis. Indeed, in accurate analyses, meshes need to be refined or rezoned until the solution converges to a value so that the error is below a predetermined tolerance. A-posteriori methods use error indicators, developed by using the theory of interpolation and approximation theory, for mesh refinements. Some use other criterions, such as strain energy density variation and stress contours for example, to obtain near optimal meshes. Although these methods are adaptive, they are expensive. Alternatively, a-priori methods, heretofore available, use geometrical parameters—for example, element aspect ratio. Therefore, they are not adaptive by nature. In this study an adaptive a-priori method is developed. The criterion is that the minimization of the trace of the stiffness matrix with respect to the nodal coordinates, leads to a minimization of the potential energy, and as a consequence provide a good starting mesh. In a few examples the method is shown to provide the optimal mesh. The method is also shown to be relatively simple and amenable to development of computer algorithms. When the procedure is used in conjunction with a-posteriori methods of grid refinement, it is shown that fewer refinement iterations and fewer degrees of freedom are required for convergence as opposed to when the procedure is not used. The mesh obtained is shown to have uniform distribution of stiffness among the nodes and elements which, as a consequence, leads to uniform error distribution. Thus the mesh obtained meets the optimality criterion of uniform error distribution.

17. Key Words (Suggested by Author(s)) Finite element Mesh refinement Stiffness matrix	18. Distribution Statement Unclassified – Unlimited Subject Category 37

19. Security Classif. (of this report) Unclassified	20. Security Classif. (of this page) Unclassified	21. No of pages 108	22. Price* A06